Advances in Colloid and Interface Science 305 (2022) 102684

Contents lists available at ScienceDirect

Advances in Colloid and Interface Science

journal homepage: www.elsevier.com/locate/cis

Review of droplet dynamics and dropwise condensation enhancement: Theory, experiments and applications

Xin Wang [a,1], Bo Xu [a,1], Zhenqian Chen [a,b,c,*], Davide Del Col [d], Dong Li [f], Leigang Zhang [e], Xinzhu Mou [a], Qiusheng Liu [g], Yang Yang [h], Qian Cao [h]

[a] School of Energy and Environment, Southeast University, Nanjing, PR China
[b] Key Laboratory of Energy Thermal Conversion and Control of Ministry of Education, School of Energy and Environment, Southeast University, Nanjing, PR China
[c] Jiangsu Provincial Key Laboratory of Solar Energy Science and Technology, School of Energy and Environment, Southeast University, Nanjing, PR China
[d] Department of Industrial Engineering, University of Padua, Italy
[e] School of Energy and Mechanical Engineering, Nanjing Normal University, Nanjing, PR China
[f] School of Energy and Power Engineering, Zhengzhou University of Light Industry, Zhengzhou, PR China
[g] Key Laboratory of Microgravity, Institute of Mechanics, Chinese Academy of Sciences, Beijing, PR China
[h] Engineering and technology center for space applications, Chinese academy of sciences, Beijing, PR China

ARTICLE INFO

Keywords:
Droplet wetting
Self-jumping
Self-migration
Dropwise condensation
Advanced functional surface

ABSTRACT

Droplet dynamics and condensation phenomena are widespread in nature and industrial applications, and the fundamentals of various technological applications. Currently, with the rapid development of interfacial materials, microfluidics, micro/nano fabrication technology, as well as the intersection of fluid mechanics, interfacial mechanics, heat and mass transfer, thermodynamics and reaction kinetics and other disciplines, the preparation and design of various novel functional surfaces have contributed to the local modulation of droplets (including nucleation, jumping and directional migration) and the improvement of condensation heat transfer, further deepening the understanding of relevant mechanisms. The wetting and dynamic characteristics of droplets involve complex solid-liquid interfacial interactions, so that the local modulation of microdroplets and the extension of enhanced condensation heat transfer by means of complex micro/nano structures and hydrophilic/hydrophobic properties is one of the current hot topics in heat and mass transfer research. This work presents a detailed review of several scientific issues related to the droplet dynamics and dropwise condensation heat transfer under the influence of multiple factors (including fluid property, surface structure, wettability, temperature external field, etc.). Firstly, the basic theory of droplet wetting on the solid wall is introduced, and the mechanism of solid-liquid interfacial interaction involving droplet jumping and directional migration on the functional surfaces under the various influencing factors is discussed. Optimizing the surface structure for the local modulation of droplets is of guidance for condensation heat transfer. Secondly, we summarize the existing theoretical models of dropwise condensation applicable to various functional surfaces and briefly outline the current numerical models for simulating dropwise condensation at different scales, as well as the fabricating techniques of coatings and functional surfaces for enhancing heat transfer. Finally, the relevant problems and challenges are summarized and future research is discussed.

1. Introduction

Droplet dynamics and condensation phenomena are the fundamentals for various technological applications in a wide range of industries such as energy utilization, seawater desalination, petrochemical engineering, agricultural irrigation, aerospace thermal management and pharmaceuticals, etc. With the rapid development of interfacial materials science, microfluidics and micro/nano manufacturing technologies, as well as the continuous in-depth study of traditional knowledge involving flow and heat transfer, research work related to the dynamic evolution of liquid drops and enhancement of condensation has been a tremendous increase in the 21st century.

In contrast to the liquid-phase fluids with large characteristic scales,

* Corresponding author at: School of Energy and Environment, Southeast University, Nanjing, PR China.
E-mail address: zqchen@seu.edu.cn (Z. Chen).
[1] The authors contribute equally

https://doi.org/10.1016/j.cis.2022.102684
Received in revised form 21 March 2022
Available online 29 April 2022

Nomenclature

θ	Contact angle [°]
ΔW	Adhesion hysteresis work [J]
r	Surface roughness
R	Radius [m]
D	Diameter [m]
Δt_c	Droplet-surface interaction time [s]
n	Droplet number
v	Impacting velocity [$m \cdot s^{-1}$]
q	Heat transfer rate [W]
ΔT	Subcooling degree [K]
h_i	Interfacial heat transfer coefficient [$W \cdot m^{-2} \cdot K^{-1}$]
G	Growth rate [$kg \cdot s^{-1}$]
h_{fg}	Latent heat [$kJ \cdot kg^{-1}$]
h_p	Micropillar height [m]
Q	Heat flux [$W \cdot m^{-2}$]
N_c	Nucleation density [m^{-2}]
$N(R)$	Size distribution of larger droplets
$n(R)$	Size distribution of smaller droplets

Greek symbols

γ	Interfacial tension [$N \cdot m^{-1}$]
φ	Solid fraction
μ	Viscosity [$kg \cdot m^{-1} \cdot s^{-1}$]
ρ	Density [$kg \cdot m^{-3}$]
τ	Contact time [s]
β	Spreading factor
λ	Thermal conductivity [$W \cdot m^{-1} \cdot K^{-1}$]
δ	Thickness [m]

Subscripts

e	Equilibrium
S	Solid phase
L	Liquid phase
V	Vapor phase
a	Advancing
r	Receding
W	Wenzel
C	Cassie
cri	Critical
b	Liquid bridge
max	Maximum
min	Minimum
p	Micropillar arrays

Abbreviations

SHS	Superhydrophobic surface
Oh	Ohnesorge number
LB	Lattice Boltzmann
Re	Reynolds number
We	Weber number
CFD	Computational fluid dynamics
NCG	Non-condensable gas
MD	Molecular dynamics
VOF	Volume of fluids

the droplet size are sometimes just a few millimeters, micrometers and nanometers, allowing the significant manipulations of droplet behaviors caused by interfacial tension, viscous stress and capillary force. In the meantime, the coalescence-induced jumping and directional migration of droplets are accompanied by deformation or even topological changes at the liquid interface, thus the different dynamic behaviors of droplets show the huge complexity. Another characteristic of droplets is the complex wetting behaviors on the advanced functional surfaces during the phase change heat transfer. The multiscale dynamics of droplet nucleation, growth, deformation and detachment are closely related to interfacial energy and surface topography. In the process of condensation, condensate droplets are concentrated in the certain populations at the solid-liquid interface. And the various dynamic behaviors such as merging, jumping and shedding occur randomly among droplet populations at each specific location. Condensation heat transfer, accompanied by convective heat transfer for phase change with the absorption and release of large amounts of latent heat, is a highly efficient way. According to the surface morphology and wetting state of droplets, vapor condensation can be classified into two modes: filmwise condensation and dropwise condensation. Due to its excellent heat transfer performance compared to filmwise condensation, dropwise condensation and its enhancement mechanism have attracted much attention. However, limited by the complex multiscale characteristics of dropwise condensation and the current levels of scientific and technological development, it is still difficult to understand the condensation process in depth and comprehensively. In the last two decades, a deeper understanding of complex multiscale dynamics of condensate droplets and its multifactorial characteristics has been achieved through the combined approaches of theoretical analysis, simulations and experiments. Actually, the current dropwise condensation has involved the fluid mechanics, interfacial mechanics, heat and mass transfer, thermodynamics, reaction kinetics and other disciplines, which have given rise to various scientific problems, such as heat transfer at the gas-liquid or solid-liquid interfaces, droplet growth and wetting transition, full-cycle multiscale dynamics from droplet nucleation to departure and multifactorial multiphysics field coupling problems.

In this work, the dynamic behaviors of liquid drops and the theory, simulations and experiments of dropwise condensation are briefly and systematically summarized, and graphical depiction of the framework and ideas is shown in Fig. 1. Firstly, the droplet wetting states and transitions on the solid substrates are outlined. Secondly, a comprehensive review of self-jumping behaviors induced by condensate droplets coalescence on the various superhydrophobic surfaces (SHS) is presented. The influence of different factors on droplet jumping, such as wettability, surface structure, fluid properties, droplet volume, coalesced number, position arrangement and size mismatch are concluded in detail. Thirdly, recent process in directional migration of droplets on the chemical and structural gradient surfaces is reviewed. Fourthly, the rebound and fragmentation behaviors of droplets after impacting the SHS are summarized. The limits of droplet contact time reduction with the addition of various microstructures are discussed. From the perspective of droplet dynamics and solid-liquid interfacial interaction mechanism, the characteristics of droplet dynamic behaviors under different conditions are summarized and analyzed. As well, the droplet modulation strategy based on the interfacial effect is discussed. Finally, we concentrate on a systematic overview of the theoretical modeling, numerical simulations and experimental studies of dropwise condensation. The various surface modifications performed to maintain efficient and continuous drop condensation are highlighted. The advantages and disadvantages of each surface fabrication are pointed out and the possibilities of their commercial applications are discussed. This review will provide the readers with a comprehensive understanding of the dynamic behaviors of droplet as well as enhanced strategies for dropwise condensation on the advanced functional surfaces.

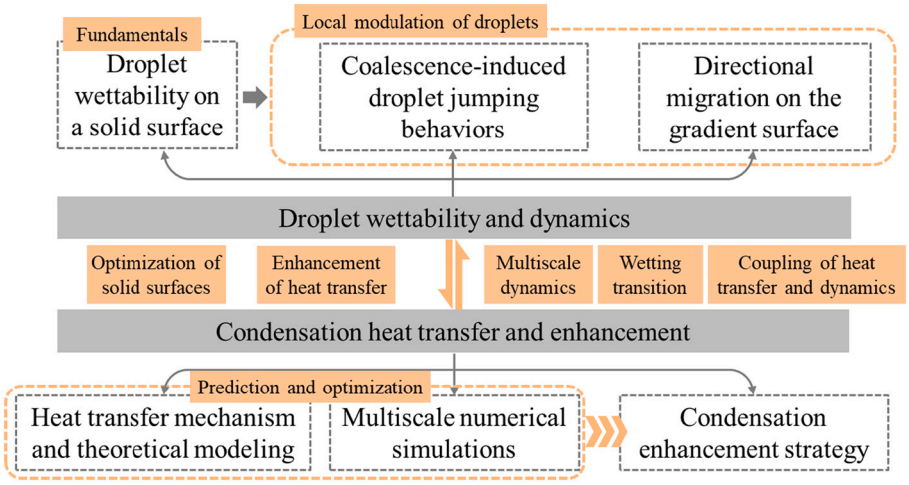

Fig. 1. Graphical depiction of the framework and main ideas

2. Droplet wettability on a solid surface

2.1. Contact angle

As the liquid contacts a solid wall, the initial gas-liquid or solid-gas interface will be replaced by the solid-liquid interface, which is known as wetting phenomenon. Wetting is the capability of liquid and solid wall to maintain the contact, a result of intermolecular interactions as they are combined. It is determined by the relationship between the adhesion and cohesion. The adhesion between the liquid and solid substrate allows the drops to spread on the solid substrate, while the cohesion inside the liquid causes the droplets to form balls to avoid contact with the surface.

Usually, the contact angle is adopted to introduce the wettability of a drop on a solid wall. Young [1] first proposed the equilibrium contact angle to describe the force equilibrium at the three-phase contact line on an absolutely smooth substrate, expressed as:

$$cos\theta_e = (\gamma_{SV} - \gamma_{LS})/\gamma_{LV} \quad (1)$$

where θ_e is the equilibrium contact angle of a drop on a smooth substrate, as illustrated in Fig. 2(a). The parameters γ_{SV}, γ_{LS} and γ_{LV} represent the interfacial tensions between gas-solid, liquid-solid and gas-liquid, respectively (the subscripts S, V and L are the solid, vapor and liquid phases). Generally, it is considered as hydrophilic surface with $\theta_e \leq 90°$, hydrophobic surface with $90° < \theta_e \leq 150°$ and SHS with $\theta_e > 150°$ and $\alpha < 5°$. The contact angle, as a reflection of force balance of droplet, is affected by the bulk force. When the solid surface is inclined, the gravitational force causes the droplet morphology to deviate from the spherical defect shape, as shown in Fig. 2(b). As the tilted angle α is large enough, the droplet will roll or slide along the solid wall. And the minimum tilted angle satisfying this condition is defined as the rolling angle. The corresponding dynamic contact angles as the droplet rolls down are the advancing θ_a and receding θ_r contact angles. The difference between θ_a and θ_r is defined as the contact angle hysteresis [2], which reflects the energy dissipation induced by droplet movement, and is often closely related to the more straightforward adhesion hysteresis work ΔW: $cos\theta_r - cos\theta_a = \frac{\Delta W}{\gamma_{LV}}$.

2.2. Wetting states and transitions

In fact, the wetting behaviors of drops on a solid substrate are more complex, and the contact angle is insufficient to characterize the actual wetting states of droplets. For the rough surface, different theoretical models have been proposed, among which two widely adopted models are the Wenzel and Cassie-Baxter models [3–5], as seen in Figs. 2(c, d). This subsection provides a brief description of two wetting models and the wetting transitions.

In accordance with the Young's equation, Wenzel investigated the wetting behaviors of droplets on the rough and porous surfaces. Considering the surface roughness, Wenzel [3] reported that the

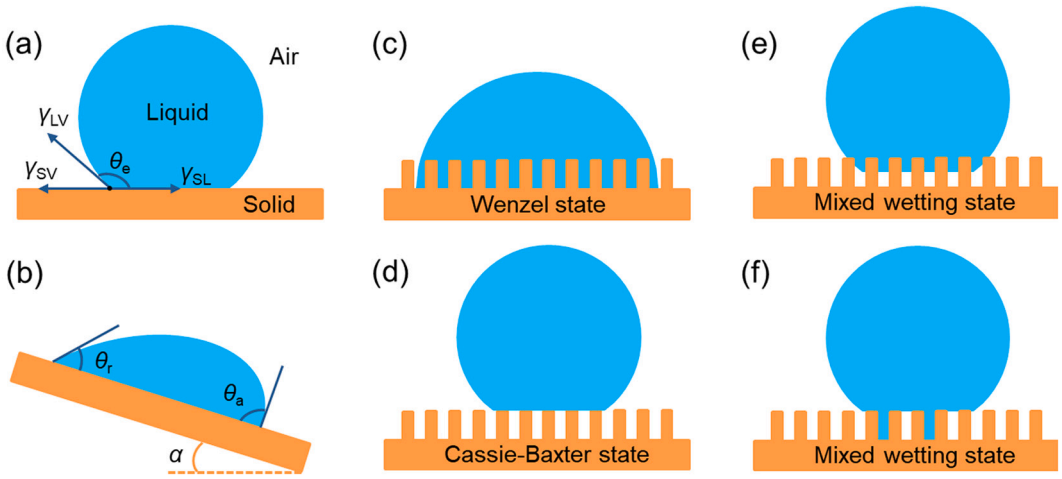

Fig. 2. Wetting modes: (a) a droplet on a flat solid wall; (b) dynamics contact angle; (c) Wenzel state; (d) Cassie-Baxter state and (e, f) mixed wetting state.

presence of surface microstructure causes the effective area between solid and liquid to be much higher than that on a flat surface. Assuming the complete contact between the droplet and rough surface, without any air pockets at the solid-liquid interface, the apparent contact angle of drop in a fully Wenzel state is given by:

$$cos\theta_W = rcos\theta_e \quad (2)$$

where r denotes the surface roughness, defined as the ratio of effective solid-liquid contact area to the projected area of droplet on the rough surface (r>1). According to Eq. (2), for the hydrophilic surface, θ_W decreases with a larger roughness, indicating the stronger wettability; while for the hydrophobic surface, θ_W increases with a larger roughness, showing the weaker wettability. Cassie and Baxter [4] suggested that all the droplets are not always in the ideal Wenzel state. The air cavities may exist between the drop and solid substrate. The Cassie-Baxter model can be described as:

$$cos\theta_C = \varphi_s(cos\theta_e + 1) - 1 \quad (3)$$

where φ_s is the solid fraction. Although Eq. (3) has been criticized by some researchers, it is still the basis for the analysis of chemically and structurally heterogeneous surface wettability [6,7]. Recently, the Cassie-Baxter equation considering the complex morphologies of the bionic surfaces was modified [8–10]. Furthermore, the Wenzel and Cassie-Baxter models are insensitive to the shape and volume of droplets as well as to the external fields (i.e., gravitational field). Actually, the case of completely Cassie or Wenzel states rarely occurs [11–13]. Miwa et al. [11] and Marmur [12] discussed the mixed wetting state of droplets, where the drops partially wet the side of the humps or part of the micropillars, and part of the droplets are located above the air pockets, as shown in Figs. 2(e, f). The actual apparent contact angle is calculated as:

$$cos\theta_{MW} = r\varphi cos\theta_e + \varphi - 1 \quad (4)$$

where φ is the percentage of projected area of solid surface wetted by the droplet. When φ=1, Eq.4 becomes Eq.2. Wong and Ho [14] considered the possible crucial effect of line tension on nanostructured relief. The detailed derivation of Eq.4 can refer to Ref. [15]. Note that, Eqs. (2-4) are applicable provided that the droplet radius is considerably greater than the surface heterogeneous characteristic scale.

As a matter of fact, various wetting states may coexist on a heterogeneous substrate. The diversity of apparent contact angles is easier to be understood when considering that the Gibbs energy profile of droplets on real surfaces exhibits multiple minimal characteristics [16–18]. Cassie impregnated states also exist in real surfaces [19,20], where the liquid penetrates into the gaps of micro/nano structures. The Cassie impregnated state possibly exists as the contact angle satisfies $cos\theta_{cri} > \frac{1-\varphi_s}{r-\varphi_s}$. For any rough surface, $\varphi_s < 1$ and $r > 1$. As a result, θ_{cri} is always greater than 90°. The Cassie state is more stable when $\theta_a > \theta_{cri}$, while the Wenzel state is more stable when $\theta_a < \theta_{cri}$. The surface hydrophobicity fails as the droplet transits from Cassie state to Wenzel state. Besides, the apparent contact angle is dominated by the local wetting state adjacent to the three-phase contact line [7]. The wetting transition is not only determined by the macroscopic wettability equation, but also nanoscale effect plays a decisive role in it. The combination of structure and wettability at different scales can be utilized to modulate the droplet dynamics at each scale, which in turn permits precise modulation of the droplet in different dynamic behaviors.

3. Coalescence-induced droplet jumping behaviors

Multi-droplets systems, as highly dispersed liquid phases, are characterized by extremely high interfacial energy compared to continuous liquid phase of the same volume. As two or more droplets approach each other and come into contact, the merging behaviors will occur driven by the local additional pressure imbalance. At this moment, the surface energy of the dispersed system will be converted into kinetic energy of droplets, viscous dissipation and solid-liquid adhesion energy. In 2009, Boreyko and Chen [21] first found that due to the weak interfacial adhesion of SHS, condensate drops can spontaneously jump off the SHS induced by coalescence in the process of dropwise condensation, as depicted in Fig. 3(a). As two or more droplets are close to each other and come into contact, a merging phenomenon occurs driven by a local imbalance of additional pressure. At this moment, the droplet surface energy gets converted into other forms of energy such as viscous dissipation energy and kinetic energy. Generally, the jumping behaviors caused by droplet merging can be subdivided into the following stages [22–24]: (a) the formation and expansion of liquid bridge before reaching the first quasi-equilibrium state, (b) acceleration of the merging droplet due to the counteraction of the non-wetting surface, (c) coalesced droplet jumping off the surface and (d) deceleration of jumping droplet in the air, as shown in Fig. 3(b). It has been suggested in the published literatures that surface tension, viscous and inertial forces play an extremely important role in droplet merging, where one of these forces is dominant will determine which mechanism the coalesced droplet undergoes. Currently, the mechanism of droplet coalescence can be classified as: viscous regime, inertial regime and inertial limited viscous regime (Fig. 3c) [25,26]. It is generally described by the dimensionless liquid bridge length $R^* = R_b/R$ and Ohnesorge number ($Oh = \frac{\mu_l}{\sqrt{\rho_l R_l \gamma}}$), where r_b is the bridge radius. The larger the Oh number, the more dominant the viscosity is in the process of droplet merging. For the inertial regime, the surface tension-induced capillary pressure is proportional to principal curvature of axial liquid interface, i.e., $\gamma_\kappa \propto 1/d(t)$, as depicted in Fig. 3(d). At this moment, the capillary pressure is balanced with the inertial flow pressure: $\rho\left(\frac{dR_b}{dt}\right)^2 = C\gamma\frac{R_0}{R_b^2(t)}$. Hence, it can be obtained that the radius of liquid bridge is proportional to the

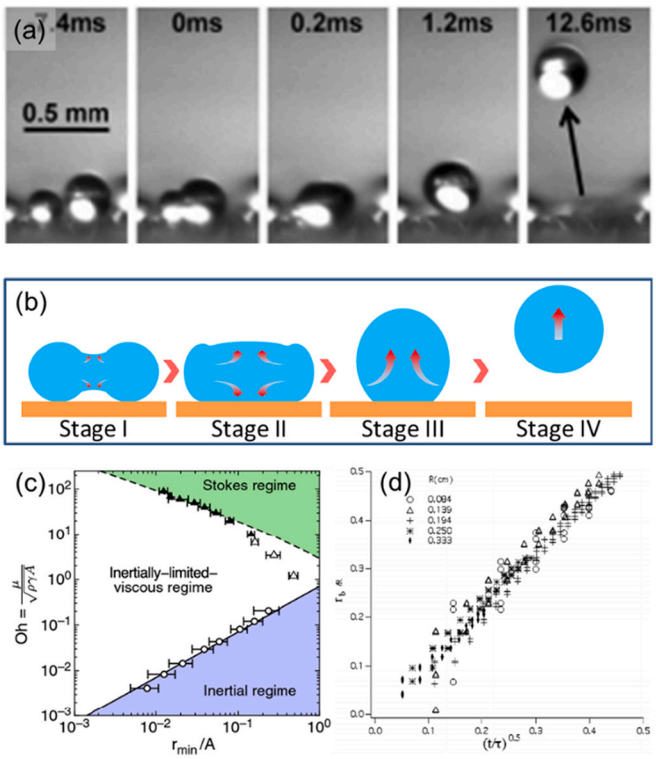

Fig. 3. (a) Self-jumping behaviors of condensate droplets induced by coalescence [21]; (b) schematic diagram of coalescence induced jumping; (c) three regimes of droplet merging: stokes, inertial and inertially limited viscous [26] and (d) bridge width of droplet versus the square root of time [28]

Table 1
Parameters affecting the coalescence-induced jumping behaviors.

Parameters	Experimental studies	Modeling studies	Comments
Wettability	Cha et al. [30]	Wang et al. [31]; Xie et al. [32]; Yin et al. [33]; Yuan et al. [34]; Li et al. [35]; Wang and Ming [36]; Wang et al. [43];	The weakening of surface wettability facilitates enhancing the jumping ability of merging drops.
Surface morphology	Liu et al. [37]; Vahabi et al. [38]; Yan et al. [39]; Wang et al. [40]; Gao et al. [41]; Yuan et al. [42];	Gao et al. [29]; Yin et al. [33]; Wang et al. [43]; Xie et al. [44]; Xie et al. [45]; Attarzadeh and Dolatabadi [46]; Zhang and Yuan [47]; Lu et al. [48]; Liu and Cheng [49];	Appropriate design of the surface structure can reduce the effective contact area between the droplet and solid wall and lessen the negative impact of contact angle hysteresis, thus improving the energy conversion efficiency.
Fluid properties	Yan et al. [39]; Vahabi et al. [50];	Farokhirad et al. [51,52]; Chen and Lian [53];	Larger surface tension and smaller viscosity decrease the jumping velocity.
Droplet volume	Cha et al. [30]; Vahabi et al. [38]; Yan et al. [39]; Vahabi et al. [50]; Chen et al. [54]; Enright et al. [55]; Zhu et al. [56];	Li et al. [35]; Dolatabadi [46]; Attarzadeh and Lu et al. [48]; Farokhirad et al. [52]; Chen et al. [53]; Wang et al. [61];	As the droplet size increases, it shifts from an inertial regime to an inertially limited viscous regime.
Merging numbers and initial arrangement	Chen et al. [54,57]; Xing et al. [60];	Shi et al. [58]; Chu et al. [59]; Gao et al. [61]; Wang et al. [62]; Wang and Ming [63]; Yuan et al. [64];	The compact droplet arrangement facilitates the jumping ability of coalesced droplets.
Size mismatch	Liu et al. [37]; Peng et al. [65]; Wang et al. [66];	Wasserfall et al. [24]; Wang and Ming [36,68]; Gao et al. [61]; Yuan et al. [64]; Wang et al. [66]; Xie et al. [67];	Size mismatch has a negative influence on the self-jumping of coalesced droplets.

square root of time [25,27–29]. For the inertial limited viscous regime, it plays a dominant role at the beginning of coalescence. However, it gradually evolves into the viscous or inertial regime at a later stage. Essentially, self-propelled droplet jumping is an inefficient energy conversion process, with only 6% of the released surface free energy throughout the process being converted into effective kinetic energy for vertical jumping. Wang et al. [62] suggested that when $Oh>0.1$ ($R>1.3$μm), the energy conversion efficiency of coalesced droplets shows a sudden drop. It indicates that the critical radius of droplet for the shift from an inertial merging mechanism to an inertial-limited viscous merging mechanism is approximately 1.3μm for isometric droplet merging on superhydrophobic surfaces. Generally, the radius of condensate droplets merging and jumping is mostly in the range of 1∼100μm. Therefore, it is universally considered that inertial effects dominate. However, it should be noted that it is unknown which force dominates and needs further study for the mismatched droplets coalescence and jumping.

Several materials in nature, such as the wings of cicadas, the skin of geckos, and the surface of lotus leaves, are natural superhydrophobic surfaces. The self-cleaning effect can be achieved by removing the dust fixed on the surface with the help of jumping induced by droplet coalescence. Since droplet merging induced jumping behaviors on the SHS was first discovered, it has attracted considerable attention in the last decade. In fact, when droplets merge on a solid surface, they are inevitably influenced by various elements, such as wettability, substrate morphology, fluid properties, droplet volume, initial arrangement and coalesced number, etc. Table 1 summarizes the published literatures on the impact of various factors on self-jumping behaviors of coalesced droplets.

3.1. Surface wettability

In fact, droplet coalescence is inevitably influenced by the surface wettability as the droplets coalesce on a solid wall. In contrast to the free droplet merging where only the growth kinetics of liquid bridges has to be considered, the droplet coalescence on a solid wall also has to take the movement of solid-liquid-gas three-phase line into account. The droplets appear perfectly spherical on superhydrophobic surfaces due to the ultra-low adhesion and extra-large contact angles. Generally, the droplet dynamics changes from spontaneous jumping to being pinned on the substrate after merging as the wettability is enhanced, which is mainly resulted from the increase of solid-liquid adhesion. The released surface energy before and after merging is decreased. As well, the efficiency of converting the excess surface energy into the effective kinetic energy of droplet is reduced. Cha et al. [30] reported the nanodroplets merging induced jumping behaviors on SHS with carbon nanotubes during vapor condensation. It was found that the minimal jumping radius of droplet increases as the advancing contact angle decreases, as depicted in Fig. 4 (b). The smallest radius of jumping drops observed experimentally was 500nm. However, the current experimental equipment cannot accurately capture the dynamic evolution of merging droplets due to the micro scale and short time. Therefore, coalescence induced jumping dynamics is mostly investigated by numerical simulations. Wang et al. [31] used the 2D lattice Boltzmann (LB) method to simulate the self-jumping induced by droplet merging on the different wettability surface, as presented in Fig. 4(a). It was concluded that the critical size of jumping drops decreases with the strengthening of surface wettability. Similar conclusions were drawn in Ref. [33, 35], as seen from the jumping velocity of merging droplets with the various contact angles and radius ratios in Fig. 4(c). In addition, other researchers studied the jumping ability of drops on the heterogeneous wettability substrate. The jumping behaviors induced by merging of two identical drops on a hybrid wettability substrate were simulated using the molecular dynamics. The results suggested that an optimal stripe width always exists to produce a maximum jumping velocity exceeding that on a 180° SHS, independent of the wettability contrast [32]. For the gradient wettability surface, the surface energy gradient reduced the droplet symmetry and caused the lower energy conversion efficiency for jumping [34]. Therefore, it can be concluded that surfaces with ultra-low contact angle hysteresis and extra-large contact angles are beneficial to enhance the jumping velocity of coalesced droplets. However, there exists a threshold of contact angle. Appropriate design of surface morphology and droplet arrangement further enhances the jumping ability.

3.2. Surface morphology

As the material science and precision manufacturing technology develop rapidly, an increasing number of researchers have tried to design and fabricate the advanced functional surfaces with different morphologies to strengthen the jumping ability of merging drops. It is possible to diminish the effective solid-liquid contact area and the negative impact of contact angle hysteresis by designing the surface structure properly, with the purpose of increasing the energy conversion efficiency optimally. The previous works showed that the spontaneous jumping of coalesced droplets is due to the liquid bridge impacting the solid surface, which causes the downward moving of part of the fluid to

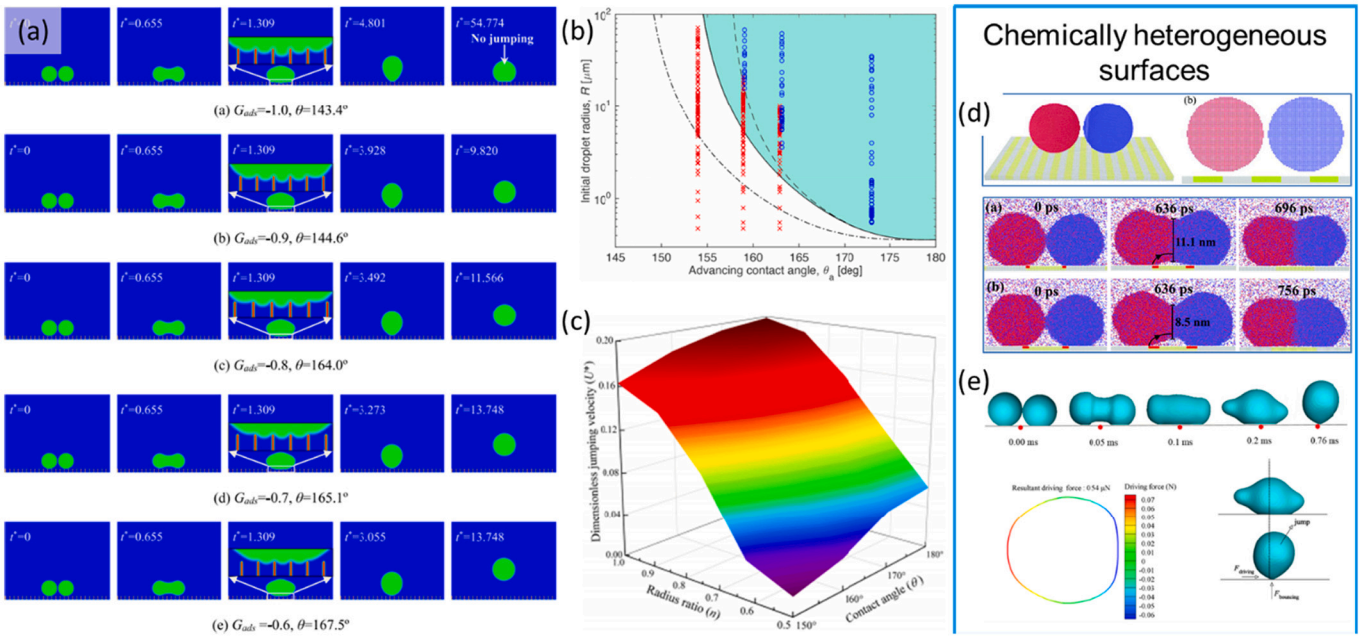

Fig. 4. (a) Dynamic evolution of droplet jumping on the various wettability surface [31]; (b) regime map of droplet jumping showing the initial droplet radius versus advancing contact angle [30]; (c) the jumping velocity versus radius ratio and contact angle [36]; droplet coalescence on the (d) hybrid wettability surface and gradient wettability surface [32,34]

change the flow direction and produce an effective kinetic energy for upward movement. Obviously, droplet impacting dynamics is related to the position of the liquid bridge impinging on the wall. As the curved liquid surface of liquid bridge partially falls into the gaps of micro-structures, it causes a decrease in the fluid changing the flow direction due to the substrate counteraction and a decline in the effective kinetic energy in the vertical direction. On the contrary, as the liquid bridge merge above the bulging structure, there exists an obvious bend in the liquid surface at the bottom of coalesced droplets. The bulging structure changes the dynamic characteristics of droplet coalescence, accelerating the contraction of solid-liquid contact area and promoting the droplets to jump away from the surface faster after merging. Therefore, a large

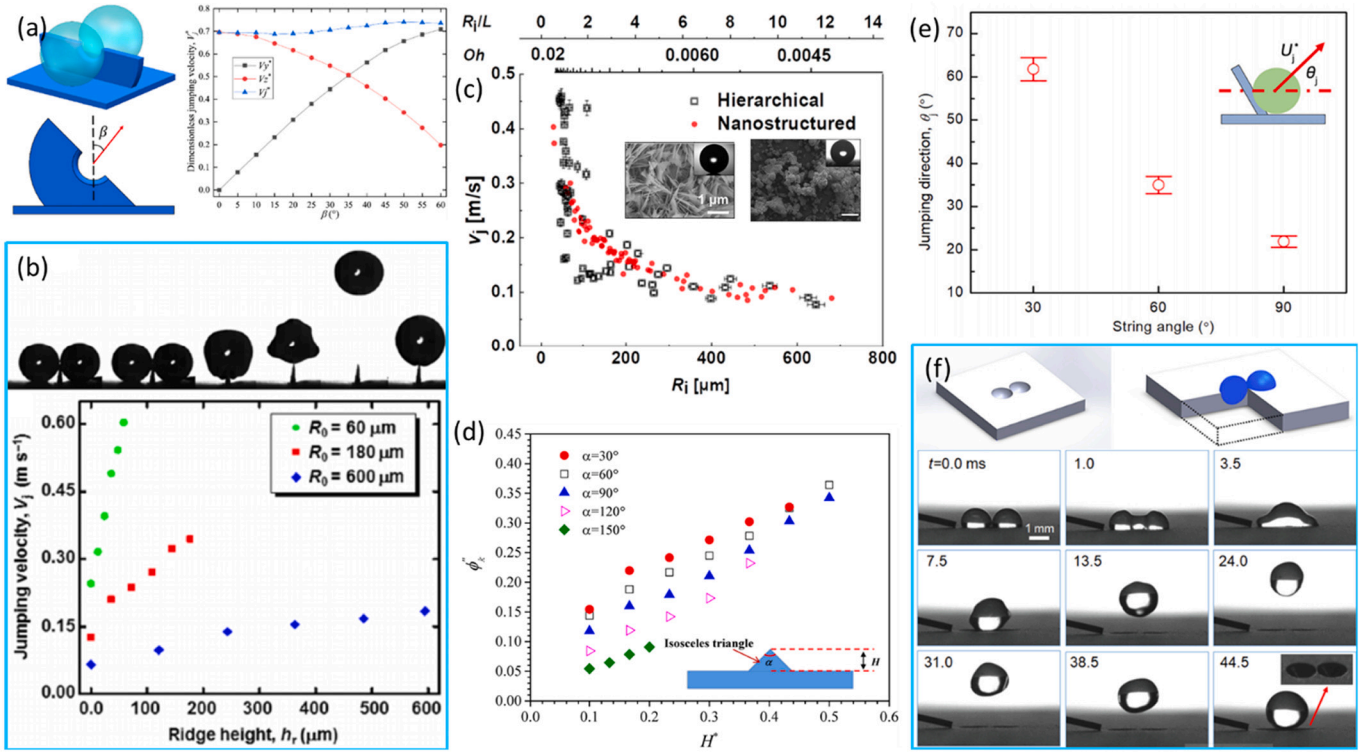

Fig. 5. (a) Droplet coalescence and jumping on the U-grooved SHS [37]; (b) self-propulsion induced by merging on the SHS with a micro-ridge [38]; (c) the jumping velocity versus droplet radius, *Oh* number as well as radius ratio [39]; (d) variation of energy conversion rate with triangular-prism structure [40]; (e) effect of the string inclined angle on the jumping direction angle [41] and (f) ultimate droplet jumping on SHS with an egg tray-like structure [42]

number of investigations have concentrated on adjusting the position of liquid bridge impinging the substrate to enhance the jumping ability of droplet. Liu et al. [37] performed an experiment of droplet jumping induced by merging on the SHS with U-shaped grooves. The energy conversion efficiency was up to 43%, as shown in Fig. 5(a). Compared with the flat SHS, the energy conversion efficiency of merging droplet was improved by ~900%. In addition, the opening direction of U-shaped groove also effected the jumping direction. The combination of SHS and macroscopic ridge structure could also significantly increase the energy conversion efficiency and induce the spontaneous jumping of drops with low surface tension and high viscosity (Fig. 5b) [38]. When the microstructure scale is significantly smaller than the drop diameter, modifying the substrate morphology hardly improve the jumping ability, as presented in Fig. 5(c) [39]. In contrast, as the microstructure size is comparable to the drop size, it is effective to improve the jumping ability and modulate the jumping direction (Fig. 5d-f) [40–42]. Certainly, the numerous researchers have optimized the substrate structure to promote the droplet jumping by the various numerical methods [29,32,42–48]. However, a quantitative analysis of how the wall structure parameters affect the specific process of droplet bouncing is still lacking, and the basis for judging the advantages and disadvantages of the surface structure is still unclear, which will be one of the main development perspectives for the enhancement of droplet jumping caused by merging.

3.3. Fluid properties

As mentioned before, coalescence induced droplet jumping dynamics can be classified into three different regimes, mainly relying on the physical properties of droplet. Until now, numerous works have reported the water droplet jumping induced by merging on the SHS. However, the self-jumping of drop with high viscosity and low surface tension has been rarely reported [39,50,53]. Compared to the oil and ethanol liquids, water with the higher surface tension is easier to form a perfect sphere on the solid wall. Yan et al. [39] conducted an experimental study of ethanol-water mixture and ethylene glycol droplets jumping induced by coalescence. For the droplets with different surface tensions, the coalescence before jumping was dominated by inertial capillary force and $\Delta t_c/\tau \approx 2.2$. For the ethylene glycol with low surface tension and high viscosity, the viscous force dominated the merging process and the droplets were pinned on the substrate after coalescence. Vahabi et al. [50] experimentally investigated the jumping behaviors of induced by droplet coalescence with the various viscosities and surface tensions on the superomniphobic surfaces. And the jumping velocity decreased with a lower surface tension and higher viscosity. In addition, variation of air inertia and viscosity surrounding the coalesced droplets had an effect on the jumping dynamics. Farokhirad et al. [51,52] investigated the influence of air inertia and viscosity on the droplet jumping using the LB method. The conclusions drawn agreed with Vahabi et al. [50]. However, how physical properties of liquid droplet and surrounding air affect droplet jumping lacks quantitative analysis, especially enhancement of the jumping ability of drops with high viscosity and low surface tension. This will be of great application to refrigerant condensation for enhanced heat transfer. In addition, the mechanism of droplet merging and jumping influenced by fluid properties is still unclear, especially the influence of surface tension on the droplet jumping dynamics still needs to be investigated in depth.

3.4. Droplet volume

A commonly applied method is to investigate the jumping height and velocity of drops with different diameters via the energy evolution before and after merging. After balancing the dissipative energy caused by solid-liquid interfacial adhesion, line tension and droplet deformation, the released surface energy of drop is eventually converted into the kinetic energy. Chen et al. [54] theoretically predicted the jumping height of droplets using a theoretical model that considered the solid-liquid adhesion, line tension and wetting states of multi-drops with different radii. Enright et al. [55] studied the coalescence induced jumping of droplets with different sizes via experiment and simulation. It was essentially inefficient that the efficiency of converting the released surface energy into kinetic energy is only 6%. To enhance the jumping ability of merging droplets, Zhu et al. [56] introduced an electric field to apply an external force to the condensate droplets. The jumping height of droplets with the diameters from 20 to 110μm was improved by more than 100% compared to that without the electric field. Wang et al. [61] studied the influence of droplet radius on the droplet jumping using a 3D LB method. A sharp drop in energy conversion efficiency at $Oh > 0.1$ ($R < 1.3$μm) was observed, indicating that for two identical droplets coalescence, the critical radius for the shift from inertial regime to inertially limited viscous regime was about 1.3μm. As well, the radius of jumping droplet is almost higher than 1.3μm. Therefore, it can be assumed that the self-jumping dynamics is dominated by inertial force. According to the dropwise condensation model, if the heat transfer needs to be enhanced, the critical removal size of droplets on the condensing surface has to be minimized. To further improve the droplet jumping condensation, finding ways to reduce the critical size of jumping droplets is necessary. It will be described in detail later in the next section: condensation heat transfer and enhancement strategies.

3.5. Coalesced number and initial arrangement

In fact, dropwise condensation involves the heterogeneous process of droplets, where the droplets of different numbers and positions constantly merge and move at the interface. When studying the multi-droplets coalescence, the initial droplet arrangement has to be taken into account, i.e., dense arrangements and discrete arrangements. Chen et al. [57] carried out the dropwise condensation on the SHS with micro/nano structures and investigated the multidroplets jumping behaviors induced by coalescence, as depicted in Fig. 6(a). It was concluded that the jumping velocity is the highest as two droplets merge. As the coalesced number increased, the jumping velocity gradually decreased, while the released surface energy was larger. Many other studies were also devoted to the self-jumping dynamics with different coalesced numbers via numerical simulations [58,59]. The more the number of merging droplets, the higher the jumping height and energy conversion efficiency converting to effective kinetic energy are. Xing et al. [60] optimized the heat transfer performance by designing a spatially heterogeneously patterned superhydrophilic- superhydrophobic substrate to precisely control the drop distribution and the coalesced numbers. Gao et al. [61] studied the impact of the coalesced number of droplets on the jumping velocity and energy conversion efficiency using the molecular dynamics method, as depicted in Fig. 6(b, c). The highest velocity of jumping droplet was observed as three drops merged, while the energy conversion efficiency decreased for an increasing coalesced number. In addition, initial arrangement of droplets could also appropriately enhance the bouncing ability. Taking three droplets merging as an example, Wang et al. [62] simulated the influence of initial droplet arrangement on the jumping dynamics using the 3D LB model, as shown in Fig. 6(d). Concentrated three droplets merging effectively improved the jumping speed compared to double droplets merging, while discrete droplet arrangement is negative for droplet jumping. Wang and Ming [63] also analyzed the self-jumping behaviors induced by three droplets coalescence with different initial arrangements (Fig. 6e). The energy conversion efficiency decreases and then increases as the distribution angle increases. The maximum value is slightly over 6.5% and the minimum value is less than 3%. To sum up, the condensing surface should be designed to promote concentrated droplet growth as well as maintain the high superhydrophobicity, inducing multidroplets to rapidly merge and jump off the surface.

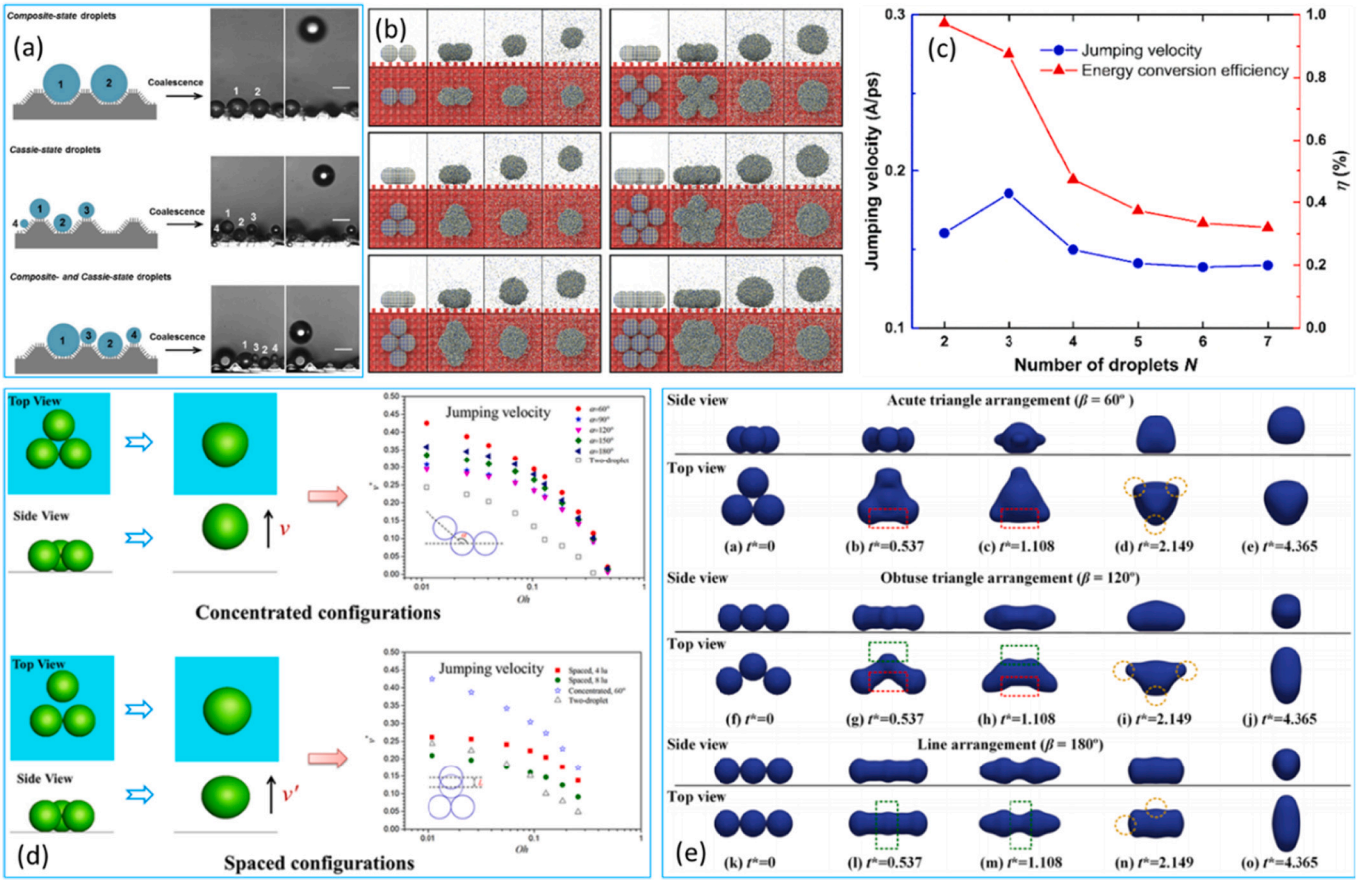

Fig. 6. (a) Merging-induced jumping of multi-droplets on the hierarchical SHS [57]; (b) dynamic evolution of the merging process between identical multi-nanodroplets (2≤n≤7) [61]; (c) jumping velocity and energy conversion efficiency as a function of coalesced number [61]; (d) effect of droplet arrangement on the jumping process [62]; (e) self-jumping behaviors induced by three droplets coalescence with different distribution angles [63]

3.6. Size mismatch

Practically, size mismatch exists between the coalesced droplets in most cases. Numerous studies [24,36,37,61,64–68] showed that the coalescence of mismatched droplets causes a decrease in the energy conversion efficiency as well as droplets impaled on the surface after coalescence. Yuan et al. [64] defined the potential for jumping and investigated the energy conversion efficiency under the various coalesced numbers, radius ratios and initial droplet arrangements. The energy conversion efficiency was higher with a greater jumping potential. The droplets were stuck to the substrate without jumping due to the jumping potential less than 0.1. Peng et al. [65] performed the droplet merging induced jumping on the microstructured SHS. Although droplet coalescence with size mismatch significantly reduced the energy conversion efficiency, the combination of microstructure and size mismatch could properly adjust the jumping angle of droplets (Fig. 7a). Wang et al. [66] studied the impact of size mismatch on the droplet jumping by experiment and simulation and the results demonstrated that non-jumping behaviors occurred at the critical size ratios below 0.56 (Fig. 7b). Xie et al. [67] reported the influence of radius ratio on the droplet jumping of coalesced droplets (Fig. 7c) and a new inertial-capillary scaling law regarding the jumping velocity was proposed. The nonjumping of mismatched drops with large radius ratios was because the large droplet swallowed the small one, thus the liquid bridge failed to impinge the solid wall. The results of Ref. [68] suggested that no jumping was observed as the radius ratio was less than 0.4, which was slightly lower than the predicted results by Wang et al. [66]. In addition, the jumping velocity reached multiple peaks as the radius ratio was below 0.7, which was different from that of identical droplets. Overall, the coalescence of mismatched droplets dramatically reduces jumping velocity and inhibits the drops jumping off the surface. When designing functional surfaces, we should try to avoid the droplet merging with large size ratios and allow as many droplets to jump off the surface as possible.

Previous works have conducted a considerable amount of theoretical, numerical and experimental studies on the droplet jumping process induced by coalescence from the various perspectives, such as the transformation form of energy, the inter-relationship between the coalesced droplets and designing and fabricating the surface morphology, etc. However, the influence of multiple variables jointly on the specific process of jumping dynamics is still unclear, and a systematic quantitative analysis is lacking. The criteria for judging the advantages and disadvantages of surface structures affecting the jumping droplet dynamics are unclear. Local modulation of droplet jumping dynamics is of great value in potential industrial applications. For example, the ultimate purpose of enhancing the jumping ability of coalesced droplets is to accelerate the removal of condensate droplets and effectively reduce the critical shedding size on the condensing surface. The local modulation of droplet jumping applied to dropwise condensation will be the main development directions in the future.

4. Directional migration of droplets on the gradient surfaces

Generally speaking, droplets appear spherical or spread along the surface in a radial manner when they contact a horizontal solid surface. However, the center of mass of the droplet remains unchanged and stationary on the solid surface. In the recent years, several methods to break the symmetry of droplets on the solid surfaces have been

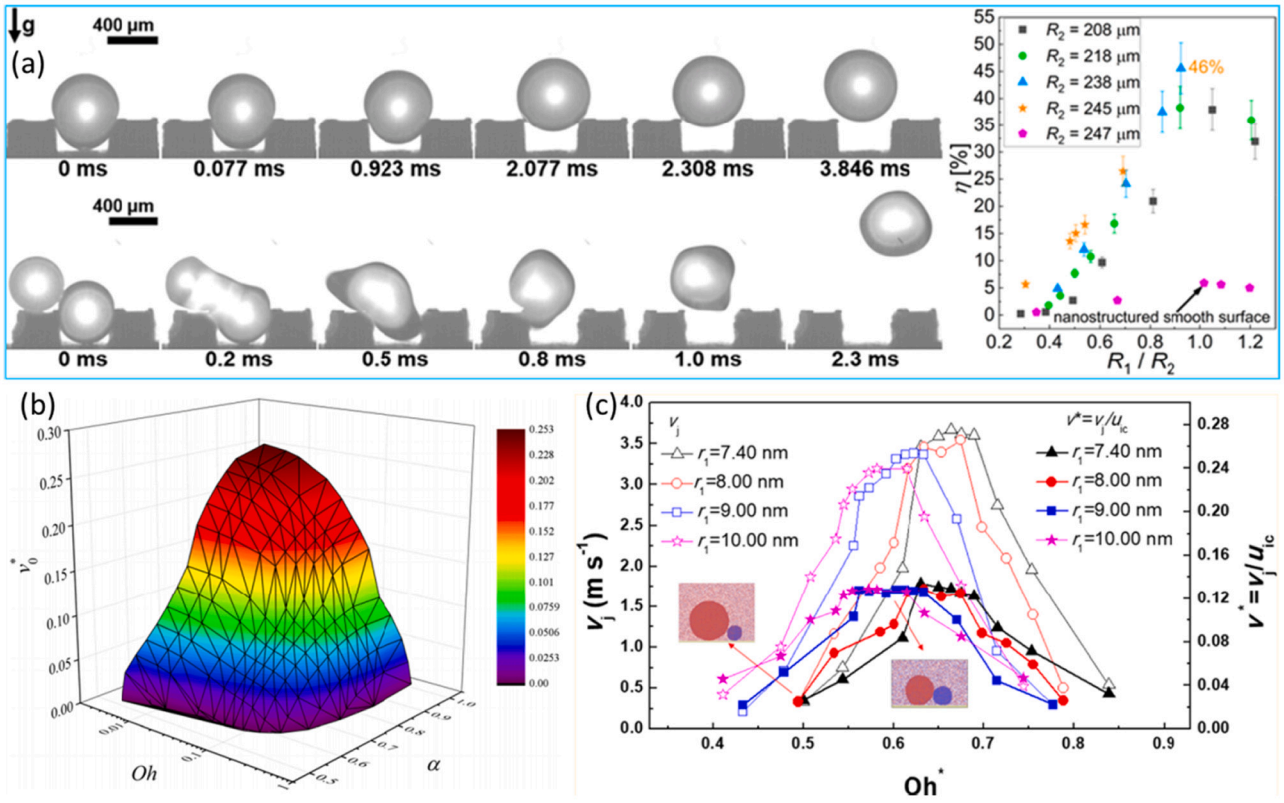

Fig. 7. (a) Variation of energy conversion efficiency versus radius ratio [65]; (b) jumping velocity as a function of size ratio and *Oh* number [66] and (c) variation of the jumping velocity versus *Oh* number [67]

developed by means of chemical gradients, structural gradients, temperature gradients, electrical gradients and mechanical vibration gradients, etc.

4.1. *Chemical gradient surface*

In terms of chemical heterogeneity, Chaudhury and Whitesides [69,70] were the first to report an experimental study of droplet movement on a wetting gradient surface. The droplet was observed to self-propelled migrate along the stronger wetting region due to the unbalanced surface tension around the droplet. This method of driving droplet self-propulsion was distinguished from thermal capillary movement and achieved by surface energy gradients from the solid surface. The fundamental reason for the droplet migration driven by the wetting gradients was the driving force generated by the combined effect of unbalanced surface tension acting on the droplet. Subsequently, a number of researchers have prepared the various wetting gradient surfaces to perform the experiments of directional migration of droplets. Daniel et al. [71] observed the droplet movement with the velocity of 1.5m/s on the wetting gradient surface in the condensation heat transfer, and the rapidly self-propelled movement of droplet could enhance the heat transfer efficiency. Subsequently, Daniel et al. [72,73] also used the vibration to eliminate the hysteresis resistance to droplet movement on the wetting gradient surface with the aim of improving the moving velocity of droplet. When the intrinsic harmonic frequency of droplet vibration matched the external forced vibration, the droplet velocity was greatly enhanced. It was found that providing a square wave vibration in the horizontal direction to droplets on a wetting gradient surface accelerates the droplet movement. Wang [74] fabricated the wetting gradient surface by silanizing the silicon surface and experimentally investigated the droplet movement on the horizontal wetting gradient surface. The droplet movement on the horizontal wetting gradient surface could be divided into two stages: accelerated movement region and decelerated movement region. As the peak velocity of droplet was relatively small and the decelerated movement region was large, the droplet movement exhibited the squirmy behaviors. In addition, for the same wetting gradient surface, the peak velocity and migrating distance of larger droplet at the same position were greater than that of smaller one. During the movement, the gas-solid interfacial energy and gravitational potential energy of droplets were reduced, and the released energy was converted into kinetic energy, gas-liquid interfacial energy, solid-liquid interfacial energy and energy dissipation of droplets. The reduction of gas-solid interfacial energy was the main reason that drives the spontaneously directional migration of droplets. Yamada and Tada [75] used electrochemical reactions of ferrocene alkanethiol monolayers to reversibly regulate the surface wettability. The wetting gradient was achieved by applying an in-plane bias voltage to the substrate. The back and forth motion of the wetting boundary, where the surface changed from the wetting to repulsion, sequentially caused the unidirectional spreading and shrinking of droplets on the surface. These unidirectional deformations led to the directional migration droplets in an inchwormlike manner.

Lai et al. [76] fabricated the surfaces with wetting gradients from superhydrophobicity to hydrophilicity (151.2° to 39.7°) via structural gradients and self-assembled monolayer gradients to induce the directional migration of droplets. Paradisanos et al. [77] and Ghosh et al. [78] fabricated the wetting gradient surfaces using the laser technique. The droplets moved at a speed of several hundred millimeters per second. Deng et al. [79] prepared the multi-wetting gradient surfaces with wedge-shaped patterns via a modified anodic oxidation method. The distance of droplet migration was controlled by adjusting the wedge angle and drop volume. As for numerical simulations, Chowdhury et al. [80] conducted a numerical study of the effective transport of glycerol droplets on a wetting gradient surface. For a constant length of wetting gradient track, the larger the wetting gradient, the larger the droplet velocity was. Li et al. [81] simulated the droplet migration on a linear

wetting gradient surface using the dissipative particle dynamics and investigated the effect of wetting gradient and droplet size on the translational velocity. Chakraborty et al. [82] studied the droplet movement on the substrate with chemical energy-induced wetting gradient by molecular dynamics. The numerical results were successfully compared with the theoretical model of droplet self-propelled movement on the gradient surface. Pravinraj and Patrikar [83] conducted a numerical study of droplet fragmentation and directional movement on the chemically heterogeneous surface using the LB method and analyzed the variation of surface free energy and the influence of contact angle hysteresis on the droplet dynamics. Lee et al. [84] also investigated the droplet migration on a wetting gradient surface using the LB method. Variation of kinetic energy, gravitational potential energy and surface energy in the process of droplet movement was analyzed. Deng et al. [85] used the free energy LB model to investigate the droplet dynamics on the wetting gradient surfaces during condensation. It was found that condensate droplets could be swept away spontaneously, thus enhancing condensation heat transfer.

4.2. Structural gradient surface

Although considerable progress has been made in the investigations of chemically heterogeneous surface, it still involves the surface functionalization of different chemical molecular gradients that may be deteriorated by the migration or oxidation of organic molecules, causing the chemical gradients to decay in long time operations. In contrast, directional transportation of droplets entirely driven by structural morphology provides a feasible strategy for solving this problem. Water droplets rolling down the stem line of rice leaves and moving on desert beetles, nepenthes and cactus spines are demonstrative examples of successful applications this principle in nature. Zheng et al. [86] prepared the wedge-shaped copper SHS combined with a PDMS oil layer to induce the water droplets movement. The unbalanced interfacial tension generated by the structural gradient provided the driving force. The superhydrophobicity greatly eliminated the droplet pinning while the smooth PDMS oil layer facilitated the droplet movement. The wetting behaviors of droplets nanostructured gradient winkle substrates were also reported [87]. After deposition of water droplets on the gradient surfaces, the different contact angles on both sides of droplets induced the self-propelled movement towards the smaller winkle size. Moreover, dynamic contact angles of droplets on these substrates increased with a larger substrate size. Wu et al. [88] investigated the oblique rebound and migration of droplets on the structural gradient surface due to the unbalanced interfacial tension generated by the heterogeneous structure. With the competition of capillary pressure and effective water hammer pressure, the self-migration of droplets towards the wetting gradient was significantly different. Liu et al. [89] designed a wetting gradient surface that could drive the droplet movement by heterogeneous structure. And the contact angle decreased from 166.0° to 15.5° with the greater pattern density. The results showed that droplets on the micropillared Silicon surfaces overcame the energy barrier to move to the stronger wettability region, while the large hysteresis resistance on the flat substrate hindered the droplet movement. In addition, multiple surfaces were designed to achieve the directional migration and long-range transport on arbitrary paths. Microstructured surfaces with wetting gradients were also prepared using photolithography and etching methods [90]. It was found that the contact angle, contact angle hysteresis and critical sliding angle increased with the increase of area fraction. The adhesion energy model of microstructured surfaces with wetting gradient was proposed based on the morphological characteristics and actual wetting area of droplets. Yin et al. [91] successfully developed a simple method based on surface microstructure to fabricate robust large-gradient surfaces, enabling selective pinning of sliding droplets. The gradients derived from microstructure changes still exhibited good mechanical properties in relatively harsh environments. Khoo and Tseng [92] fabricated the gradient surfaces with nanostructured patterns that could transport the droplets of different volumes with the speed up to 0.5m/s. The droplet velocity depended on the droplet position and gradient angle. In addition, ascension of droplets with all-round adaptability and a subnanoliter droplet movement were also demonstrated. Practical applications have also been tested based on the experimental results. Mertaniemi et al. [93] mixed two droplets at the intersection of two tracks to provide guidance for mixed bio-microfluidics. Yang et al. [94] fabricated parallel and narrowing dual-track hydrophilic tracks to control the transport, mixing and release of droplets on microfluidic chips. Compared to the directional migration of droplets on a wetting gradient surface, the moving velocity on a structural gradient surface was faster and transported over longer distances. Wetting patterned surfaces with specific structural tracks were of great significance for enhanced condensation heat transfer due to the timely and efficient condensate droplets removal. Alwazzan et al. [95] constructed the stripe patterns with different hydrophobicity on the copper tubes. The stronger hydrophobic region possessed the high mobility of droplets, and the weaker hydrophobic region allowed the droplets to move directionally along the path trajectory. The heat transfer performance was improved by 180% compared to dropwise condensation on the fully hydrophobic surface as the hydrophilic to hydrophobic width ratio was optimal. In addition to parallel wettability stripe patterns, inverted V-shaped patterns, wedge-shaped patterns, and tree-like patterns have been developed and investigated to enhance condensation heat transfer [96–98].

5. Condensation heat transfer and enhancement strategies

During the dropwise condensation, droplet modulation is closely related to the heat transfer performance. Generally, depending on the microstructure of substrate and the wettability of condensate liquid on the condensing surface, two condensation modes can be classified as filmwise and dropwise condensation. The heat transfer coefficient can be increased by more than 3 times compared to that of filmwise condensation [99–102]. In the last decade, the complex dynamic cycle of dropwise condensation and its multi-factor and multi-scale characteristics have been better understood through experimental visualization investigations, multiscale numerical simulations and theoretical analysis. Nowadays, it seems that dropwise condensation heat transfer has already involved several disciplines and generated multiple scientific problems, such as heat transfer at the gas-liquid or solid-liquid interfaces, droplet wetting dynamics, multiscale evolution of condensate droplet from nucleation to departure, as well as multi-factor multi-physics fields coupling of interface chemistry, fluid mechanics, hear transfer, materials science and imaging science, which is of great value and engineering applications. As a matter of fact, the generation and growth of droplets during condensation is a multiscale phenomenon in which the wetting mechanism is extremely complex, accompanied by the wetting state transition and complicated three-phase contact line movement. Considering the complexity of phase change problems, the mechanism of dropwise condensation is an open issue.

5.1. Heat transfer mechanism and theoretical modeling

Vapor molecules condense on the subcooled surface to form the nanodroplets and gradually grow to merge with neighboring droplets. Eventually, the droplets detach from surface by bouncing, rolling or sliding. The droplets continue to condense on the renewed substrate in cycles. An understanding of heat transfer mechanism contributes to the development of classical heat transfer models. In terms of single droplet heat transfer, the effects of gas-liquid interfacial heat transfer, thermal resistance of droplet curvature, and thermal resistance of droplet thermal conductivity are considered comprehensively. With the continuous development of dropwise numerically and experimentally, its heat transfer mechanism and theoretical modeling have also been fully developed. To predict heat transfer of dropwise condensation on

different structured surfaces, the growth rate and heat transfer of individual droplet are required to be known. Kim and Kim [103] combined single drop heat transfer and size distribution to develop a heat transfer model on a smooth hydrophobic substrate. The thermal resistance in the process of single droplet heat transfer was mainly caused by gas-liquid interface, self-heat conduction of droplet, coatings and droplet curvature. The heat transfer rate of a drop was given by:

$$q(R) = \frac{\Delta T \pi R^2 (1 - R_{\min}/R)}{\left(\frac{\delta}{\lambda_{\text{coat}} sin^2\theta} + \frac{R\theta}{4\lambda_c sin\theta} + \frac{1}{2h_i(1-cos\theta)}\right)} \tag{5}$$

where ΔT was the surface subcooling degree and $R_{\min}$ was minimum droplet radius. λ_{coat} and δ were the thermal conductivity and thickness of hydrophobic coating. λ_c and h_i denoted the thermal conductivity of droplet and interfacial heat transfer coefficient, respectively. Assuming a constant angle for droplets with different radii, the growth rate of single droplet was expressed as:

$$G = \frac{\Delta T}{2\rho h_{\text{fg}}} \frac{1 - R_{\min}/R}{\frac{R\theta(1-cos\theta)}{4\lambda_c sin\theta} + \frac{\delta(1-cos\theta)}{\lambda_{\text{coat}} sin^2\theta} + \frac{1}{2h_i}} \tag{6}$$

where h_{fg} is the latent heat caused by phase change. For a practical structured condensing surface, the contact angle varies with droplet growth. Therefore, variation of the contact angle versus droplet radius was modeled to give the heat transfer rate of a drop on a micropillared substrate covered with hydrophobic coating [104]:

$$q(R) = \frac{\Delta T \pi R^2 (1 - R_{\min}/R)}{\frac{R\theta}{4\lambda_c sin\theta} + \frac{1}{2h_i(1-cos\theta)} + \frac{1}{\lambda_{\text{coat}} sin^2\theta}\left(\frac{\lambda_p \varphi}{\delta\lambda_p + h_p\lambda_{\text{coat}}} + \frac{\lambda_c(1-\varphi)}{\delta\lambda_c + h_p\lambda_{\text{coat}}}\right)^{-1}} \tag{7}$$

where h_p and λ_p were the height and thermal conductivity of micropillar arrays. φ was the solid fraction. The corresponding growth rate of droplet was written as:

$$G = \frac{\Delta T}{2\rho h_{\text{fg}}(1 - cos\theta)^2(2 + cos\theta)} \frac{1 - R_{\min}/R}{\frac{1}{2h_i(1-cos\theta)} + \frac{R\theta}{4\lambda_c sin\theta} + \frac{1}{\lambda_{\text{coat}} sin^2\theta}\left(\frac{\lambda_p \varphi}{\delta\lambda_p + h_p\lambda_{\text{coat}}} + \frac{\lambda_c(1-\varphi)}{\delta\lambda_c + h_p\lambda_{\text{coat}}}\right)^{-1}} \tag{8}$$

With a large number of applications of lubricant infused porous surface for enhanced the heat transfer, Maeda et al. [105] estimated the heat transfer of a droplet. The thermal resistance of lubricant was added compared to the micropillar structured surface. The above three computational models of a drop heat transfer are applicable to the most condensing surfaces.

Combining the droplet size distribution and heat transfer rate related to surface structure, the overall heat flux in the steady state was obtained [106]:

$$Q = \int_{R_{\min}}^{R_{\text{cri}}} q(R)\text{n}(R)\text{d}R + \int_{R_{\text{cri}}}^{R_{\max}} q(R)\text{N}(R)\text{d}R \tag{9}$$

where R_{cri} was the droplet radius upon interaction, related to the nucleation density N_c. $R_{\max}$ was the maximum shedding radius of droplet. Generally, condensate droplets during condensation can be divided into two groups: smaller droplet with $R_{\min} < R < R_{\text{cri}}$ and larger droplet with $R_{\text{cri}} < R < R_{\max}$. Le Fevre and Rose [107] derived the size distribution of larger droplets as:

$$N(R) = \frac{1}{3\pi R^2 R_{\max}} \left(\frac{R_{\max}}{R}\right)^{2/3} \tag{10}$$

The size distribution of smaller droplets was given by:

$$n(R) = \frac{1}{3\pi R_{\text{cri}}^3 R_{\max}} \times \frac{R_{\text{cri}} - R_{\min}}{R - R_{\min}} \times \frac{A_2 R + A_3}{A_2 R_{\text{cri}} + A_3} \times \left(\frac{R_{\max}}{R_{\text{cri}}}\right)^{2/3} \times exp(B_1 + B_2) \tag{11}$$

where the parameters A_2, A_3, B_1 and B_2 could be found in Ref. [108].

Liu and Cheng [109,110] studied the free energy barrier considering the temperature distribution of droplets via thermodynamic analysis to obtain the nucleation radius and density of droplets. The nucleation radius and nucleation density of droplets obtained theoretically are used as input parameters for the classical dropwise condensation heat transfer model. In addition, the effects of surface wettability, subcooling degree, coating thickness and thermal conductivity on the heat transfer were considered. As different types of SHS are widely used in dropwise condensation, heat transfer models considering various factors have been proposed. From the perspective of the condensate droplet removal mode, Xie et al. [111] modeled the various shedding modes of drops and analyzed the maximum size of droplets on the nanostructured SHS for the various departure modes: self-jumping, rolling and sliding. The condensation heat transfer model considering the various shedding modes was developed by reasonably selecting the droplet shedding radius and nucleation density. The introduction of nanostructures increased the nucleation density and droplet population, which facilitated the dropwise condensation heat transfer. However, the additional thermal resistance caused by the nanoporous layer deteriorated the heat transfer performance. In addition, a model of condensation heat transfer on biphilic substrates was developed. The optimal width of hydrophobic stripe was governed the coating thickness and the width of hydrophilic stripe. The condensation heat transfer was enhanced by 67% maximally compared to a completely hydrophobic surface [112]. Undoubtedly, the effect of droplet merging and bouncing was still important. The model of heat transfer from a droplet was modified to acquire a new function of droplet size distribution [113]. Recently, a model of single droplet heat transfer containing non-condensable gases (NCG) has also been developed. In contrast to the pure vapor condensation, droplet heat transfer was divided into wet air to condensing surface and heat transfer through the droplet. In the analysis of mass transfer process, the computational area could be divided into the Knudsen layer and the continuous flow area. The molecular dynamics theory and the continuous medium theory were adopted respectively, the influence of droplet size and non-condensable gas was considered comprehensively. For the heat transfer process, Fourier's heat conduction law was used. The droplet growth rate, nucleation size and temperature distribution were obtained under different conditions. As various novel wettable surfaces have been proposed, condensation heat transfer on the heterogeneous wettable substrates has been developed [114–116]. Singh et al. [115] introduced the influence of wetting gradient and merging behaviors on the droplet departure, and the proposed model agreed well with the experimental data. Biomimetic hydrophilic-hydrophobic surfaces, as an efficient heat transfer surface, have also attracted much attention. Shang et al. [116] developed the condensation heat transfer model on a hydrophilic- hydrophobic substrate and predicted the transition from filmwise to dropwise condensation by considering the droplet dynamic characteristics during the droplet growth and shedding, effectively revealing the physical mechanism of enhanced condensation heat transfer on a biomimetic surface.

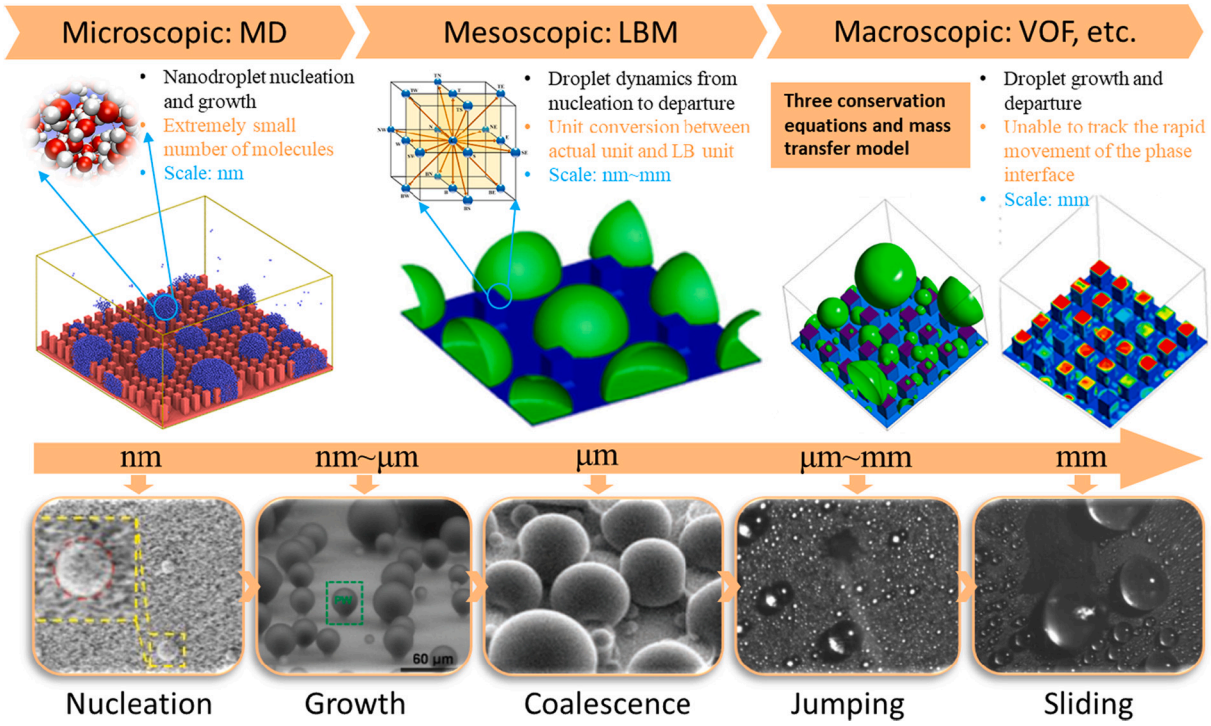

Fig. 8. Multiscale numerical methods from microscopic to macroscopic for simulating dropwise condensation [123,131,148,194,224]

5.2. *Multiscale numerical simulations from microscopic to macroscopic*

Dropwise condensation is a multiscale dynamic evolution and thermal-mass transport process across interfaces, where energy-mass transport at the liquid-gas and solid-liquid interfaces plays a significant role. Considering its complexity, both theoretical modeling and experiments are greatly limited. Numerical simulations are gradually becoming an effective investigative tool. In this section, numerical methods in the various scales, shown in Fig. 8, will be briefly summarized in three main categories: microscopic molecular dynamics (MD), mesoscopic LB model and other traditional CFD methods.

5.2.1. *Molecular dynamics method*

Previously, MD method was used to study the various interfacial problems. Although condensation can only be carried out in nanoscale via MD method, the generation and wetting of nanodroplets has an irreplaceable role in the subsequent growth of droplets. In addition, it provides a deeper insight into the microscopic mechanism. At present, it has been extensively applied to investigate the mechanisms of initial droplet formation and wetting state modulation as well as to explore the feasible mechanism for nanodrop removal. Kimura and Maruyama [117] obtained the droplet nucleation rate, critical nucleation radius and nucleation free energy via MD simulations. The results revealed that MD simulation results agreed well with the heterogeneous nucleation theory as the subcooling degree was small or the surface wettability was weak. The condensate modes on the various wettable surfaces and the effect of surface tension on the nanodrop dynamics and film formation were also investigated [118]. According to the classical nucleation theory and numerical results, the formation mechanisms of different condensation modes were revealed and dropwise condensation was the transient state from non-condensation to filmwise condensation. By analyzing the dynamic evolution of "similar liquid film" in the process of condensation, the mechanism of droplet formation was usefully supplemented. Niu and Tang [119] reported the influence of surface wettability on the heat transfer of condensation in nanochannels. The higher heat transfer efficiency of filmwise condensation than dropwise condensation in nanoscale was due to the lower interfacial thermal resistance between the condensate and hydrophilic substrate. The analysis of different wettability surfaces revealed that at the solid-liquid interface, the temperature jump was larger and the interfacial thermal resistance was higher on the hydrophobic surface, which showed an opposite characteristic of condensation heat transfer at the macroscopic scale. Besides, the influence of NCG on condensation was investigated, and different modes of wetting transitions with the corresponding NCG content or subcooling degree were acquired [120]. The nucleation and growth of droplets on the nanostructured surface was also simulated [121]. Decreasing the spacing of nanopillar and increasing the heat flux led to the growth of droplets in the upper part of nanopillars, which agreed with that reported by Huang et al. [122]. And a lubricant infused surface was proposed to recover the droplet Cassie state [123]. Gao et al. [124] studied the influence of micropillar structures on the wetting dynamics and droplet growth. As the solid fraction decreased, nanodroplets presented Cassie state, partial Wenzel as well as Wenzel state sequentially on structured substrates. Wetting transitions as well as dewetting behaviors were observed in the process of formation, growth and merging of nanodroplets. For the water condensation on variable wettability surface, the stronger wettability promoted the condensation rate [125]. On the hydrophobic surface, water molecules or small water clusters, as the potential nucleation sites, tended to escape to the gas phase when encountering the surface. Xu and Chen [126] modeled the water condensation on a composite wettability wedge shaped surface, where the wedged shape and wettability gradient promoted the departure of condensate droplets.

5.2.2. *Lattice Boltzmann method*

Due to the natural parallelism and the advantages of dealing with complex boundaries, the mesoscopic LB model has been developed as an excellent and effective tool for simulating condensation heat transfer. It mainly includes pseudopotential model, color model and free energy model, among which the pseudopotential model is most widely used in simulating phase change problems. The kinetic modeling and mesoscopic properties of LB model determine its potential not only to reflect macroscopic physical phenomena but also to simulate microscopic interactions. Liu and Cheng [127] firstly studied the laminar film

condensation on a subcooled vertically hydrophilic surface via thermal LB pseudopotential method with two distribution functions. the thickness and velocity of liquid film as well as temperature distributions under steady conditions was obtained. The simulation results agreed well with classical analytical results. Moreover, dynamic evolution of condensate droplets and variation of departure size with gravitational force were investigated. And the change of heat flux with time was calculated for the first time using the LB method [128]. Subsequently, their team also investigated the transition from dropwise condensation to filmwise condensation on the mixed wettability substrates. In addition, a multicomponent multiphase LB model was developed to simulate the effect of NCG content on forced convective filmwise condensation [129–131]. The LB method applicable to the complex boundary conditions has been applied. Based on the hybrid thermal LB model [132,133], Li et al. [134] firstly considered the effect of NCG on the vapor condensation. The presence of NCG decreased the heat flux and condensation rate, increased the waiting time before nucleation and cycling time from nucleation to departure. For the vapor condensation on hybrid wettability substrates, the results suggested that the ratio of the width of hydrophilic to hydrophobic region corresponding to the maximum heat flux is different as the mass fraction of NCG varies [135]. Wang et al. [136] also performed numerical simulations of vapor condensation on the downward facing heterogeneous wettability substrates. When the hydrophobic-hydrophilic ratio was small, the heat transfer performance was deteriorated in contrast to dropwise condensation on a completely hydrophobic substrate. For the various wetting difference, the optimal heat flux corresponding to the hydrophobic-hydrophilic ratio was different. Subsequently, the influence of surface morphology and structural parameters on condensation heat transfer was investigated, and the coalescence induced droplet jumping on the microgrooved and microspined surfaces coupling with the phase change heat transfer was simulated [137–139]. Considering the effect of NCG, droplet jumping condensation was also investigated. The diameter and maximum jumping height of coalesced droplet decreased with a larger NCG content [140]. The increase in subcooling degree accelerated the condensate growth rate and facilitated a higher jumping height.

5.2.3. Other CFD methods

Traditional numerical models (e.g., VOF and Level set) have been well modeled and analyzed for filmwise and flow condensation [141–146]. The VOF methods are built on the Lee model [147] or a delta function of heat flux at the interface to calculate the mass source caused by phase change. Although the Lee model is easily implemented in commercial software, it is built according to the temperature difference with the saturated temperature instead of the interfacial temperature gradient, and the relevant coefficients rely on the specific problem. In spite of the delta function of heat flux without any coefficients, the accuracy of VOF model needs to be improved because the average thermal conductivity of liquid and gas phases is chosen. For another, the Level-set method is based on the interface-diffusion model. However, it is ineffective to calculate the filmwise condensation when the interface thickness is larger than liquid film thickness. The above two simulation methods have common drawbacks: it is particularly challenging to capture the rapidly moving interface and calculate the heat and mass transfer through the interface, especially for dropwise condensation. Recently, Ke et al. [148] developed a transient 3D VOF model to study the condensation modes on the various wettability substrates. Droplet jumping condensation on the SHS and the heat flux as a function of time were successfully simulated. Of course, new numerical methods have also been proposed to accurately simulate the dropwise condensation. Jiang et al. [149] combined the chemical gas-liquid absorption theory and pure vapor condensation model to propose a new method for calculating the dropwise condensation in the presence of NCG. Effects of *Re* number and surface subcooling on the dropwise condensation was investigated. It was revealed that the heat flux is highest at a contact angle of 133°. Hu et al. [150] proposed a 3D event-driven multiscale for modeling dropwise condensation. The dynamic octree data structure and related algorithms were used to improve the computational efficiency. The effect of droplet departure mode on heat transfer was discussed. When droplets detached mainly by droplet jumping rather than sliding, droplet coverage on the surface was smaller while droplet density and heat flux were larger. Macner et al. [151] reported a new method to simulate transient dropwise condensation and reasonably predicted the time evolution of droplet population density, fractional coverage, normalized condensate volume and median droplet radius. The condensation process probably started with nucleation at the fixed sites and transitioned to random nucleation as more and more favorable sites were activated.

5.3. Condensation enhancement strategy

In the last century, the investigations of dropwise condensation concentrated on measuring the heat transfer coefficients under different conditions and exploring the variability between different results. With the widespread acceptance of the classical heat transfer model proposed by Rose et al. [152], heat transfer mechanism and the measurement of condensation coefficient have been solved, whereas limited by the time-dependent property of dropwise condensation. Up to now, filmwise condensation is still widely existed in most of condensers. Therefore, the heat transfer efficiency is extremely limited and needs to be improved. With the rapid development of micro/nano fabrication technology, a large number of researchers have designed and prepared highly reliable, low surface energy condensing surfaces for experimental studies, and combined with environmental scanning electron microscopy (ESEM) and high-speed camera for microscopic observation of the dynamic behaviors of condensate droplets. Currently, an increasing number of surface structures and coatings have been used to improve the heat transfer, such as inorganic compounds, precious metals, polymers, surface alloys and organic compounds, etc. Design and preparation of advanced functional condensing surfaces with low surface energy based on conventional SHS is one of the hot topics in dropwise condensation. In particular, for the dropwise condensation in the presence of NCG, the critical nucleation radius was increased, resulting in the formation of initial droplets being more difficult and placing higher demands on the design and optimization of relevant surface modification techniques. In this section, the different categories of SHS fabrication technologies are summarized.

5.3.1. Coatings

The initial proposed approach to enhance the heat transfer of dropwise condensation is utilizing surface coatings, which typically deposit a thin coating material of low surface energy on the condensing surface. The thickness of coating is essential to maintain the dropwise condensation heat transfer. A thinner coating presents the stable dropwise condensation for a long time due to its oxidation and moisture absorption. However, the thicker the coating, the greater the corresponding thermal resistance is, which has a negative impact on heat transfer.

5.3.1.1. Polymer coatings. In industrial condenser applications, combining cost and performance, PTFE and other fluoropolymers are an effective way to promote dropwise condensation. Among all polymeric materials, PTFE and other fluoropolymers are most widely used. It has been shown that the heat transfer performance is significantly enhanced with PTFE and fluoropolymer coatings in contrast to the filmwise condensation on the metallic substrates [153–155]. Recently, the thickness of fluoropolymer coatings was reduced to 780nm after using the dip-coating technique [156]. The heat flux and heat transfer coefficient were improved by 26% and 15% respectively. To ensure the durability of coatings, Ma et al. [157,158] used Ar^+ and N^+ ion beams to obtain the better adhesion of coatings. The heat transfer performance was only slightly reduced for 500 hours of continuous operation on a

copper substrate. For the brass tube coated with PTFE, the heat transfer coefficient and heat flux were increased by 1.6-28.6 times and 0.3-4.6 times compared to the filmwise condensation. Even after continuous operation for 340 hours, the heat transfer coefficient was enhanced by 100%. Paxson et al. [159] reported the stable dropwise condensation on a thin film of poly-(1H, 1H, 2H, 2H-perfluorodecyl acrylate)-co-divinyl benzene p(PFDA-co-DVB) grafted to a metal substrate using initiated chemical vapor deposition method. In contrast to the silane coatings, the substrate was rougher and more nucleation sites were formed. The heat transfer coefficient was improved by over 7 times compared to the filmwise condensation, and stable dropwise condensation was maintained for continuously operating over 48h. In addition, this substrate could be used to achieve enhanced dropwise condensation of fluids with low surface tension such as ethanol, hexane and pentane [160]. However, to further increase the durability of the polymer requires a larger thickness, but the increase in thickness leads to an increase in thermal conductivity and thermal resistance, which is detrimental to heat transfer. Therefore, suitable bonding materials and methods between thin polymer layers and substrates can be sought to reduce the thermal resistance and improve the heat transfer capability. It was also a promising approach that the combination of polymers and other materials to form composites improves the thermal conductivity of coatings by dispersing more particles or thermally conductive phases into coatings. PTFE nanoparticles covered with metal substrate enhanced dropwise condensation due to higher thermal conductivity than PTFE [161]. Chang et al. [162] reported the superior durability and high thermal conductivity of composite metal and polymer coatings compared to the pure polymer coatings. Ni or P composite with PTFE was also used to enhance the heat transfer of dropwise condensation [163]. It revealed that the capillary pressure generated at the solid-liquid interface in the process of condensation causes the delamination of coatings [164]. However, it is still a challenge to obtain coatings with thin thickness and good durability that can sustain dropwise condensation for a long time. In-depth understanding of the coatings of the causes of coatings failure and damage will facilitate the optimized surface design and enhanced heat transfer.

5.3.1.2. Noble metals. Despite the high surface energy to promote the liquid film formation, noble metals exhibit a similar "hydrophobicity" that enhances dropwise condensation. In comparison to the polymer coatings, noble metals are of high thermal conductivity. Nevertheless, because the noble metals are extremely expensive, the required amount of material for the coatings is crucial. Woodruff and Westwater [165] plated the gold coatings of different thickness on the copper surfaces by electrodeposition. The coating had little effect on enhancing dropwise condensation for the thickness less than 20nm, while it was significantly effective for the thickness over 200nm. According to the report of Smith [166], dropwise condensation was observed on the copper surface only with a minimum thickness of 100nm for the gold coating. Ge et al. [167] plated 15-50μm thick gold on stainless steel plates by electroplating. The increase of NCG concentration deteriorated the heat transfer. At high concentration of NCG, the gold-coated surfaces showed no superior heat transfer performance. Similarly, silver coatings were also be applied to the condensing surface via electrodeposition method. O'Neill and Westwater [168] measured the heat flux up to 1.5MW/m^2 on the sliver-coated surface. The heat transfer coefficient was enhanced by 57.72% when active agent was added to the silver-coated surface. Besides, the durability was better compared to the pure silver coating [169].

5.3.1.3. Rare earth oxides. In earlier years, lanthanide rare earth oxides (REOs) were showed to exhibit the hydrophobicity and enhance dropwise condensation [170]. Compared to the organic polymers or noble metal coatings, the shedding diameters and cycling time of condensation on the REOs surfaces were smaller. The researchers have also developed a method for forming praseodymium oxide, cerium oxide, gadolinium oxide, holmium oxide, lanthanum oxide and terbium oxide coatings on micro/nano structures that can be textured by laser etching, spraying or colloidal processes, with the films gradually deposited on the substrate to create the superhydrophobicity. Khan et al. [171] fabricated the condensing surface with a CeO thin film coating, which maintained the dropwise condensation after 100h of continuous operation. And the heat transfer coefficient was improved by 10 times over filmwise condensation. The surface could also be superhydrophobic by covering the metal surface with a CeO coating less than 200nm thickness by wet chemical treatment, and the heat transfer coefficient was 5 times greater compared to that of the silane-coated surface [172]. However, the heat transfer performance, durability and robustness of such coatings need to be further investigated.

5.3.1.4. Self-assembled molecules (SAMs) coatings. Using surface molecular self-assembly technology, a stable single-molecule layer film is formed by spontaneous interactions between molecules and substrate through non-covalent bonding forces. One end of the monolayer film is anchored to the substrate by chemical bonding, while the other end features functional groups with low surface energy that maintain the excellent hydrophobicity. Since the thickness of coating is only a few tens of angstroms, the thermal resistance of SAMs is negligible and the amount required is very small and low cost [173,174]. It has been demonstrated that silane-based SAMs exhibit better durability and stronger bonding compared to thiol-based SAMs, and therefore are used in more studies [175]. Das et al. [176] studied the copper-nickel and copper tubes with cetyl mercapton SAMs for a pioneering study of condensation, exhibiting the enhanced heat transfer performance. Wen et al. [177] prepared a layer of SAMs on a copper surface. Although dropwise condensation was observed, the heat transfer performance was greatly diminished after the coating deterioration. Vemuri et al. [178] comparatively investigated the durability of stearic acid and n-octadecanethiol SAMs coated on the copper tubes. The stearic acid coating reduced the contact angle from 155° to 61.1° after 10h of continuous operation, while the n-octadecanethiol coating maintained the good hydrophobicity after 100h of continuous operation and the contact angle decreased to 111.2° after 2600h. Borner [179] reported that the lifetime of thiol-based SAMs exceeds 9 months and the heat transfer performance was improved 10 times compared to filmwise condensation. The surface energy of docosanoic acid monomolecular layer was lower than that of the Ni-P-PTFE coating and the heat transfer coefficient was over 10 times higher in comparison with that of the filmwise condensation [174]. To prolong the durability of SAMs, self-healing coatings were proposed to increase the effective lifetime [180,181]. Molecular self-assembly method has been increasingly applied in dropwise condensation due to the low thermal resistance and simple procedures. Due to its extremely small self-assembled film thickness (~nanometer scale), its robustness, corrosion resistance and durability need to be further investigated.

5.3.1.5. Graphene and CNT coatings. Low- and atmospheric-pressure CVD methods are most extensively applied for graphene coating to produce ultra-thin graphene coatings on the copper tubes [182]. The condensation heat transfer coefficient of graphene-coated surface is four times over that of the bare copper surface (3.5~5K). Moreover, dropwise condensation can be maintained for two weeks of operation. However, it is impossible to enable graphene coatings to be superhydrophobic due to the lower advancing and receding angles. Besides, the processing cost of grapheme is extremely expensive, which limits its application. However, the cost issue will be resolved accordingly with the optimization and development of coating technology.

The high thermal and chemical stability as well as hydrophobicity of carbon nanotubes has contributed to the development in condensation applications. Generally, CNT SHS were fabricated by spraying [183], post-spraying heat treatment [184], CVD [185] and dip coating [186].

Chen et al. [187] obtained a lotus-like superhydrophobic surface by depositing CNTs using the Cr-Ni layer as a catalyst, whereas the cetyl alcohol-coated surface was more durable than the CNTs coated surface. Besides, heat transfer was also enhanced by 60% on the steel substrate with MWCNT/Fe composite coatings [188]. Although CNTs coatings exhibit the higher heat transfer performance, the droplets are easily pinned at high subcooling the heat transfer performance is deteriorated substantially. Although these emerging surface coatings are capable of maintaining a stable dropwise condensation mode, the development of these coatings is still in the early stage. More mature processing techniques are required to implement the practical applications.

5.3.2. *Micro/nano structured substrate*

In the previous section, we have discussed the surface modification techniques based on different coatings. Different materials are coated on the substrate mainly to reduce the surface energy to improve the dropwise condensation heat transfer. Interestingly, highly disordered condensate droplets can be modulated by changing the surface morphology. Even though the purpose pf applying the coating is to reduce the surface energy, the condensate droplets cannot be removed by gravity and grow to the diameter that is comparable to the capillary length (water droplet: ~2.7mm). The thermal resistance of large droplets is high, causing the deterioration of condensation heat transfer. It has been found that the design and fabrication of various surface morphologies can reduce the removal size pf droplets. As we have discussed in section 2.2, adding the micro/nano structure can greatly increase the droplet contact angle. Surely, the mobility of condensate drops depends on the wetting states. As the micro/nano fabrication techniques develop rapidly, micro- and nano-structures are designed by a great number of methods, such as etching [189], laser [190], electrodeposition [191], and 3D printing [192]. The substrate is further hydrophobized after being coated with low surface energy materials. Depending on the surface roughness, it can be generally divided into nanostructured and hierarchical micro/nano structured surfaces.

5.3.2.1. Nanostructured surface. Nanostructured SHS with single layer of roughness are commonly used in vapor condensation on account of the self-jumping induced by droplets merging that enhances condensation heat transfer [21]. The departure diameter of condensate droplets can be significantly reduced by designing the nanostructures appropriately. Miljkovic et al. [193,194] prepared knife-shaped nanostructured copper SHS and performed the vapor condensation outside the copper tubes, observing the merging-induced jumping dynamics of condensate drops, as depicted in Fig.(9a). The heat flux and heat transfer coefficient were improved by 25% and 30% respectively than those of the advanced hydrophobic substrate. Wen et al. [195] studied the wetting transition mechanism of condensate drops on the tapered nanostructured SHS at the different subcoolings. As the subcooling degree was less than 0.3K, condensate drops with Cassie state detached from the surface by self-bouncing behaviors. As the subcooling degree exceeded 0.6K, the decrease of nucleation radius and the increase of nucleation density caused the nucleation and growth of nanodroplets in the nanostructure gaps and resulted in the superhydrophobicity failure and deterioration of heat transfer performance. To investigate the influence of nanopillar size on condensation heat transfer, SHS with the various nanopillared structures were fabricated (Fig. 9b), and the critical jumping diameter of condensate drops was found to be strongly dependent on the height, diameter and spacing of nanopillar [196]. Tall and slender nanopillars were found to induce 2μm droplet jumping, while the minimum jumping diameter of droplets on short and thick nanopillars were over 20μm. Xie et al. [197] focused on the effect of operation time on dropwise condensation on the nanograssed SHS. After one week of continuously operation, not only was the heat transfer deteriorated, but also the original droplet jumping condensation changed to the conventional

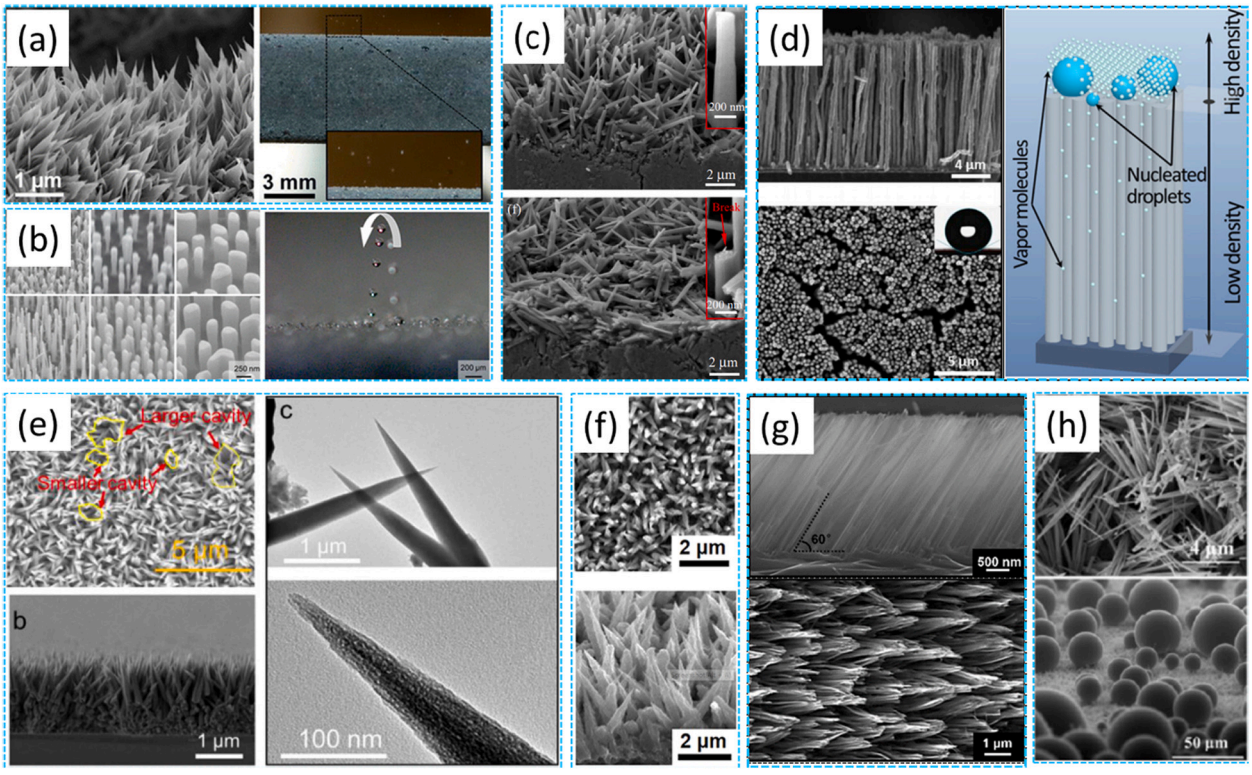

Fig. 9. (a) Droplet jumping condensation on knife-shaped nanostructured SHS [193]; (b) SHS with the various nanopillared structures and Tall and slender nanopillars promote the smaller droplet jumping [196]; (c) the collapse and fracture of the nanograssed structures after long-time condensation [197]; (d) 3D superhydrophobic nanowire networks [199]; (e) silicon nanowire SHS [200]; (f) the copper SHS with nanocones [201]; (g) titled nanowires [202] and (h) nanocone arrayed SHS [203]

dropwise condensation. The collapse and fracture of the nanograssed structures were seen from SEM images in Fig. (9c). However, the droplet growth rate was much higher than the removal rate at the large subcooling, leading to the condensate flooding the substrate. To eliminate this problem, Wen et al. [198] fabricated the hydrophobic copper surface with nanowires and achieved the ~100% higher heat flux at the subcooling degree up to 24K. Besides, droplet jumping condensation on a 3D copper nanowire SHS (Fig. 9d) was observed as the subcooling was 28K and the 100% higher heat flux was enhanced [199]. The silicon nanowire SHS (Fig. 9e) was also prepared by Lu et al. [200] to reduce the droplet shedding diameter, and condensation heat transfer was enhanced compared to the hydrophobic surface at both small and large subcoolings. In addition to nanowires, several investigations of condensation on nanoconical surfaces have been carried out. The copper SHS with nanocones, as shown in Fig. 9(f), were prepared using an electrodeposition method [201]. Although the heat transfer performance was enhanced for the vapor at low temperature, it was deteriorated for the vapor at low temperature (80°C), mainly caused by the sharp increase in droplet nucleation density and growth rate. They also found that titled nanowires (Fig. 9g) generate the asymmetric surface tension and microdroplet merging release the driving energy conductive to self-jumping removal and heat transfer enhancement [202]. Jin et al. [203] fabricated the SHS with nanocone arrays using chemical bath reactions and silane modification, as shown in Fig. 9(h). The condensate droplets were preferentially nucleated in the cavities and then extruded to be Cassie state, and eventually removed by self-jumping. To sum up, both nanowires and nanocones exhibit diminished heat transfer performance for high temperature steam at large subcoolings due to the vapor penetration and a dramatic reduction in nucleation size.

5.3.2.2. Hierarchical micro/nano structured surface. The condensation heat transfer of hierarchical micro/nano structured SHS is significantly better than that of nanostructured SHS with single roughness. Chen et al. [204] reported a hierarchical micro-pyramid and nanograss structured SHS satisfying both high nucleation density and rapid droplet removal rate, as shown in Fig. 10(a). Compared to the nanostructured SHS, the nucleation density of droplets was improved by 65% and the removal rate of droplet was accelerated by 450%. Besides, the flower-like micro/nano structured SHS was fabricated. It was found that the droplet dynamics depends on the micro-flower density. The higher the micro-

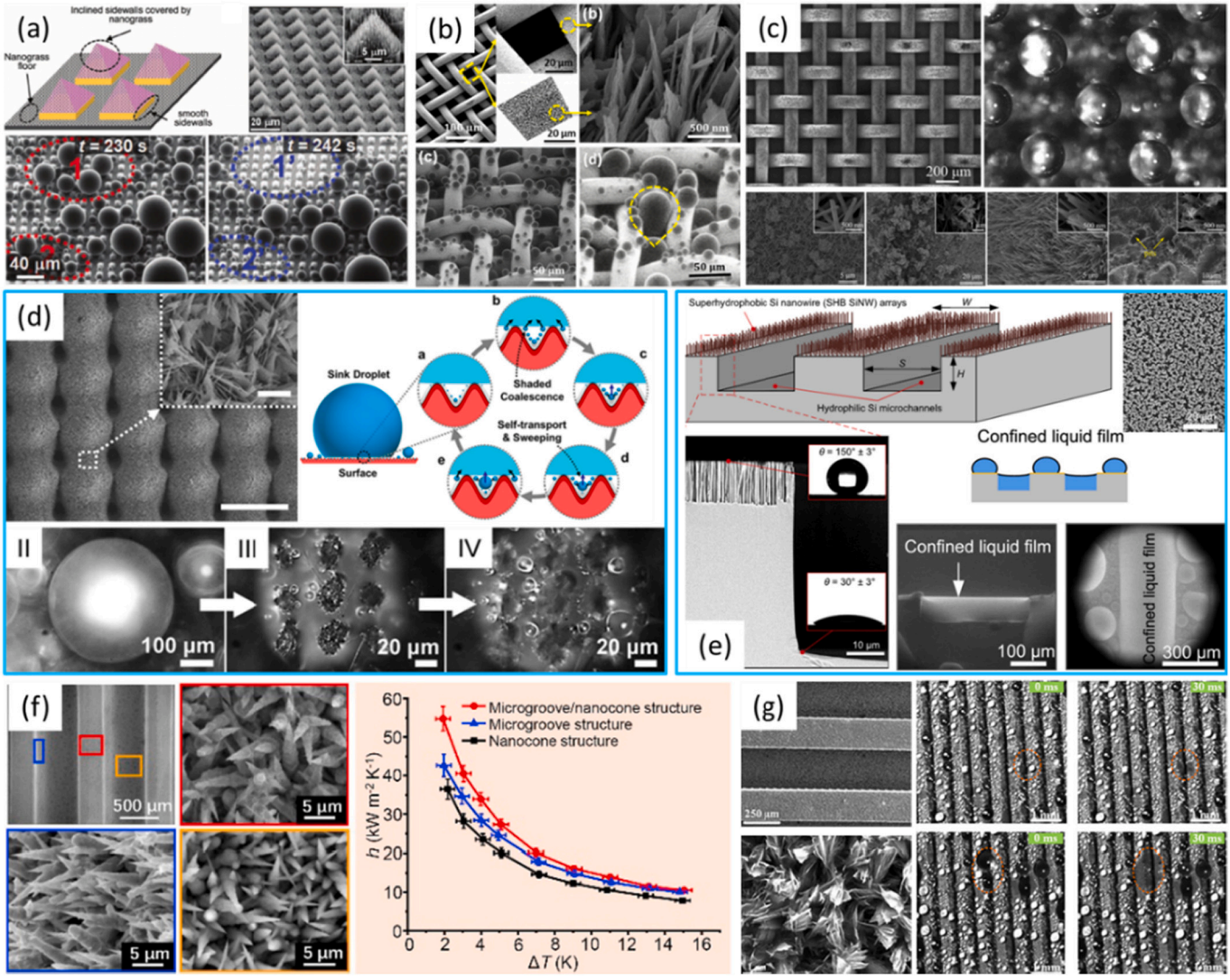

Fig. 10. (a) Schematic drawing and SEM of micropyramid-arrayed SHS with nanograsses and coalescing and self-jumping of multidroplets [204]; (b) Forced jumping of stretched drops on the microporous surface with nanoblades [207]; (c) 3D micromesh substrate with nanostructures to control the modulate the droplet nucleation [208]; (d) hierarchical condensation on the micropillared SHS with nanostructures [209]; (e) 3D hybrid wettability surface composed of superhydrophobic silicon nanowires and hydrophilic microchannels to accelerate the droplet removal [210]; (f) fabrication of the SHS with composite structures of microgrooves and nanocones to enhance heat transfer [211] and (g) hierarchical microgrooved SHS to promote the droplet self-jumping at a large surface subcooling [212]

flower density, the more the droplet nucleation sites, the smaller the critical size departure of droplets and the faster the removal frequency were [205,206]. Aili et al. [207] designed a microporous surface with nanostructures to modulate the growth, coalescence and jumping behaviors of droplets (Fig. 10b). In addition to the conventional droplet coalescence-induced jumping behaviors, forced jumping of stretched drops in pores through merging with the others outside the pores or individual self-pulling was observed. Similar 3D micromesh substrate with nanostructures (Fig. 10c) was shown to well control the nucleation of condensate droplets [208]. Properly design of micropillar arrays was additionally to achieve the hierarchical condensation to enhance heat transfer [209]. The presence of larger Cassie droplets accelerated the growth of underlying smaller droplets by 21% compared to the conventional droplet growth (Fig. 10d). Apart from the various micropillar arrays, microgrooves combined with nanostructures can also significantly improve the heat transfer performance. Lo et al. [210] proposed a 3D hybrid wettability surface composed of superhydrophobic silicon nanowires and hydrophilic microchannels (Fig. 10e). The microchannels limited the thickness of liquid film and the formed liquid bridges could be self-removed. A highly efficient heat transfer coefficient was maintained at the large subcooling, with the heat flux up to 655kW/m^2. Chen et al. [211] fabricated the SHS with composite structures of microgrooves and nanocones using wire electrical discharge machining, electroless copper plating and thiol modification technologies (Fig. 10f). By optimizing the microgroove structure, condensation heat transfer coefficient was enhanced by 82.9% in comparison with the flat hydrophobic surface, and an optimized micro/nano structured surface was superior to the nanocone structured surface. Peng et al. [212] fabricated a hierarchical microgrooved SHS by chemical etching and mechanical broaching to perform the vapor condensation (Fig. 10g). Two droplet jumping modes were observed, i.e., normal self-jumping of smaller drops at a smaller subcooling (ΔT<5K) and forced jumping of large stretched drops at the larger subcooling (ΔT<12K). At a fairly wide range of subcooling (ΔT<24K), the heat flux was 66% higher compared to the hydrophobic substrate.

5.3.3. Bionic surface

Inspired by plants or animals in nature, bionic surfaces designed through the synergistic utilization of micro/nano structures and surface chemistry are of great significance to enhance the heat transfer of vapor condensation. In recent years, efforts have been devoted to explore bionic advanced functional surfaces to implement self-removal of condensate droplets. Lv et al. [213] observed the continuous self-jumping behaviors of drops on a lotus leaf with two-layer roughness, (Fig. 11a). Surface energy dissipation and contact angle hysteresis limited the jumping size of droplets. Ghosh et al. [97] prepared alternating hydrophilic-superhydrophilic hybrid wettability surfaces inspired by banana leaf (Fig. 11b). Capillary pressure-driven droplet directional migration achieved an overall improvement in condensate collection. Feng et al. [214] designed a multi-level asymmetric structured surface inspired by pine needles. In the process of condensation, condensate droplets were transported in the direction of increasing tip height through merging, thus achieving the spontaneous removal of condensate drops, as shown in Fig. 11c. Beetle back composed of alternating hydrophobic and hydrophilic regions was reported to be superior in water collection properties [215] (Fig. 11d). Hou et al. [216] prepared a bionic SHS with high wetting contrast inspired by the desert beetles, as shown in Fig. 11e. During the condensation, the synergistic effect of the mixed wettability surface resulted in the improved performance in all aspects of droplet population density, growth rate and spontaneous removal. The heat transfer was enhanced by 63% in comparison with the silicon hydrophobic substrate. Ju et al. [217] proposed

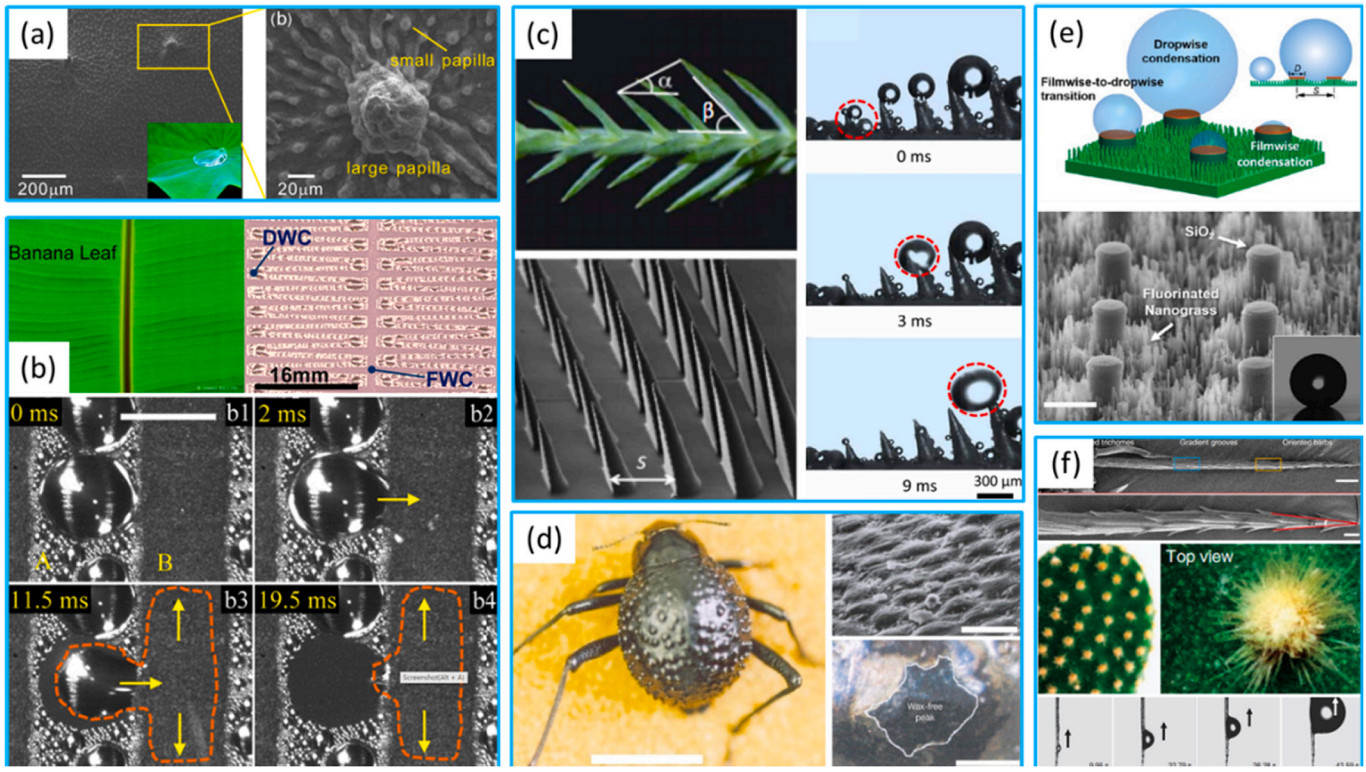

Fig. 11. (a) The lotus leaf with two-layer roughness [213]; (b) hydrophilic-superhydrophilic hybrid wettability surfaces inspired by banana leaf to induce droplet directional migration [97]; (c) the multi-level asymmetric structured surface inspired by pine needles to transport condensate droplets in the direction of increasing tip height through merging [214]; (d) beetle back composed of alternating hydrophilic and hydrophobic regions [215]; (e) a bionic SHS with high wetting contrast inspired by the desert beetles [216] and (f) a unique system of uniformly distributed cone-shaped spines and trichomes on the cactus stem to induce droplets spontaneous movement [217]

that a unique system of uniformly distributed cone-shaped spines and trichomes on the cactus stem could enhance the fog collection performance (Fig. 11f). The directional transportation of water droplets was accelerated by the Laplace pressure gradient, the surface-free energy gradient and multiple-function integration. For the bionic surfaces, the critical shedding size of droplet is smaller than the gravity-driven critical size, and the optimal condensation heat transfer performance of bionic surface can be achieved by optimizing the hydrophobic-hydrophilic ratios. This emerging work is still in the preliminary stage and the development of novel advanced bionic surfaces will receive more and more attention.

5.3.4. Lubricant infused surfaces

Droplets can easily maintain the Cassie state on a SHS. However, an irreversible Wenzel state is formed when droplets are partially penetrated into the micro/nano structures, resulting in the poor heat transfer. To solve this problem, Wong et al. [218] proposed the porous surface infused by slippery liquid to maintain the extremely low contact angle hysteresis (<2.5°) for the various and complex fluids (water, hydrocarbons, crude oil and blood) and rapidly recovered the fluid repellency (Fig. 12a). After infusing an appropriate amount of lubricant into micro/nano structured surfaces, the percentage of pinned droplets was significantly reduced and droplets down to 100μm were able to maintain a high mobility, as shown in Fig. 12(b) [219]. The high mobility provided efficient removal rate and enhanced heat transfer. Xiao et al. [220] reported the combination of reduced oil-water interfacial energy, heterogeneous surface energy and substrate structure to fabricate the functional surface (Fig. 12c). The nucleation density and high droplet removal rate were greatly increased, and the heat transfer coefficient was twice higher over the conventional dropwise condensation. Sett et al. [221] developed a nano-lubricant infused substrate of ultra-low contact angle hysteresis. Stable dropwise condensation of low surface tension liquids such as ethanol and hexane could be maintained. A 200% increase in condensation heat transfer coefficient was achieved in comparison with that of the hydrophobic surface. Guo and Tang [222] prepared the hydrophilic lubricated surface with both small contact angle and rolling angle, maintaining the high mobility of droplets and increasing the nucleation density. When the nitrogen content was 9.2%, the heat transfer coefficient was increased by 113.8-120.3% compared to the normal SHS. Besides, hydrophilic lubricant infused surfaces consisting of microchannels and nanostructures (Fig. 12d) were fabricated to accelerate the droplet nucleation and removal [223]. Although exciting results, such as rapid nucleation and high mobility of droplet, have been indicated on the lubricant infused surfaces, deterministic measurements of heat transfer enhancement are still limited and further experiments are required to elucidate the enhanced condensation heat transfer. Besides, the durability needs to be further evaluated and strengthened. Note that, for the crucial applications related to condensate quality, the presence of lubricants contaminates the condensate liquids and the practical applications can be further limited.

5.3.5. External field

When vapor condensation is implemented on these functional surfaces, enhancement of condensation heat transfer is restricted by (1) the returning of jumping droplets due to gravity, (2) convective vapor entrainment caused by the buoyancy effect of the vapor adjacent to the surface and (3) entrainment of local vapor flowing to the substrate. Improvements to this problem will not only improve the heat transfer but also ensure the efficient condensation operating for a long time. A number of additional strategies can also be adopted to enhance condensation heat transfer, such as the various waves and electric fields. Miljkovic et al. [224] found that the removal of droplets from condensing surfaces could be improved using the external field. Although the jumping frequency of drops was independent of external

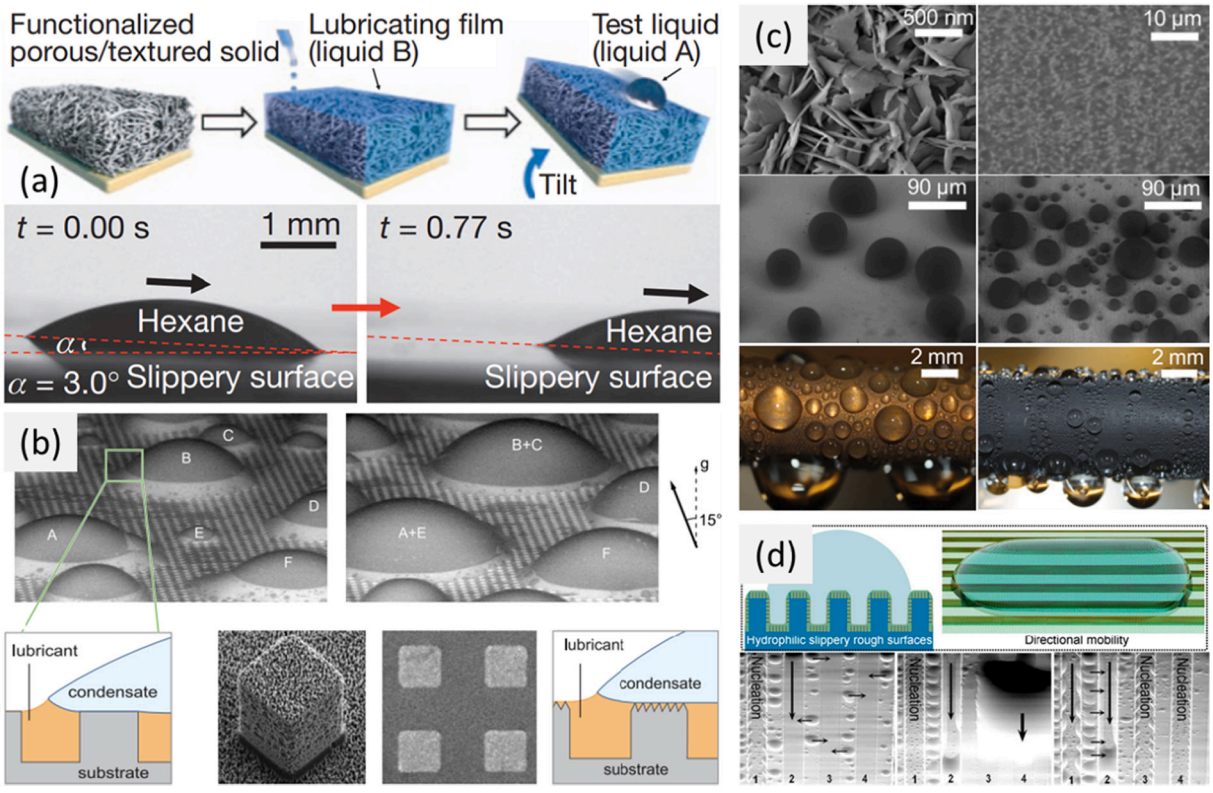

Fig. 12. (a) Schematic of the porous surface infused by slippery liquid and sliding of a low-surface-tension liquid hydrocarbon-hexane demonstrating the mobility [218]; (b) the growth of water drops on micro-post surface impregnated with BMIm [219]; (c) Comparison of droplet nucleation and departure on the nanostructured surface and oil-infused nanostructured surface [220] and (d) Fast droplet removal on the hydrophilic lubricant infused surface consisting of microchannels and nanostructures [223]

electric field, it prevented the return of jumping droplets. The overall heat transfer coefficient of condensation was improved by 50% in comparison of the absence of external electric field [225]. After applying the electric field, the maximum jumping height of droplets during condensation was increased by over 200% [226]. Wikramanayake and Bahadur [227] compared the effect of alternating current and direct current on condensation heat transfer. In contrast to the direct current, alternating current promoted the growth rate and coalescence of droplets and enhanced the heat transfer by 31%. Attempt was also made to mechanically vibrate a vertically oriented condensing surface, where condensate droplets moved and detached from the surface with smaller size and higher frequency. The heat transfer was enhanced by more than 70% at the excitation frequencies of 100Hz and 200Hz [228]. Oh et al. [229] also applied vibration driving to lubricant-infused nanoporous surfaces. The droplet mobility, controlled droplet repulsion and efficient heat transfer were enhanced. The rapid removal of drops and heat transfer improvement could be achieved controllably via a synergistic combination of surface chemistry, electric field and mechanical vibration.

5.4. Challenges

The above review provides a broad scope for further efficient and flexible modulation of the dynamic wetting behaviors of droplets during condensation. However, the complexity of functional surface preparation, the diversity of engineering applications and the marketability of engineering costs have also posed many challenges, as summarized below: (1) In-depth understand the mechanism of droplet nucleation under the influence of multiple factors and the multiscale modeling from droplet nucleation to departure. Surface morphology has an important influence on the formation of initial droplets and the transition of wetting behaviors. Although the restricted space caused by micro and nano structures is beneficial to the nucleation process, it also poses great difficulties for modeling investigations according to the classical nucleation theory. (2) Reinforce the droplet removal effect and quantitatively assess its influence on heat transfer performance. For example, the continuous application of new removal methods such as external field strengthening, droplet merging and spontaneous jumping and directional migration, how to establish the judging conditions for droplet shedding from SHS to improve the droplet size distribution model has become one of the current difficulties in theoretical modeling. (3) How to combine experiments, simulations and theoretical investigations to integrate existing results and break through relevant bottlenecks. For example, the results of molecular dynamics simulations have been unable to be applied to the improvement of relevant models. Although different research approaches have made clear process in the respective fields, the chasm between the fields is growing, causing the greater difficulties for the integration of the various results. (4) The performance of numerous functional surfaces is still limited to experimental tests and remains a long distance from practical industrial applications. In the meantime, considering the wide range of heat transfer equipment applications and the requirement for low maintenance costs, it also poses a challenge to fabricate low-cost functional surfaces for industrial applications.

6. Applications

Droplet dynamics and condensation heat transfer widely exist in a variety of industrial applications, such as energy utilization, desalination and water harvesting, petrochemicals, microelectronic cooling, thermal management systems and heating, ventilation, and air conditioning (HVAC), etc. In this section, we will further discuss the applicability of droplet dynamics and condensation heat transfer for various terminal applications.

6.1. Power plant

Currently, most of the world's electricity still relies on coal, oil and gas-fueled thermal power plants. For steam-driven power plants, a condenser is located downstream of the turbine. Condensation is achieved by a liquid-coupled shell and tube condenser, a cooling tower and an air cooler. Vapor condensation is of great importance to the efficiency of power generation in power plants. Although a variety of advanced functional surfaces for enhanced dropwise condensation have been mentioned in section 6.3, the durability of coatings and surface structures still needs to be addressed. Recent experimental studies on condensation heat transfer have been conducted on the individual surface. Despite the increased heat transfer coefficients being calculated, the heat loading capacity of the overall component is rarely reported. Ion plating technique was used on copper tubes to promote dropwise condensation [230]. Although dropwise condensation mode was observed, a comparison of the heat transfer performance of filmwise condenser and dropwise condenser is lacking. Kananeh et al. [231] reported a triple increase in heat transfer coefficient of ion implanted steel tubes. And the stable dropwise condensation could be achieved only at low rates of cooling water. The purpose of using dropwise condenser is to increase the condensation rate and power plant output and to reduce the fuel consumption. Therefore, the condenser needs to be optimized to increase the output power.

6.2. Desalination and water harvesting

Desalinated water is utilized in most water-scarce regions to augment the supply water, basically through membrane processes and thermal processes. The widely used thermal desalination technologies such as multi-stage flash distillation, multi-effect distillation and hot vapor compression rely on evaporation of brine and collection of condensate water. Dropwise condensation enhances heat transfer rates, reduces heat transfer area as well as lowers production costs. Condensation is also involved in water collection, which requires transporting water from the captured surface to a designated area. Inspired by biological surfaces such as desert beetles, cactus spines and nepenthes, researchers found that advanced functional surfaces could significantly improve the water collection efficiency.

6.3. HVAC

It is well known that typical heating, ventilation, and air conditioning systems require the use of condensers to exhaust heat to the environment, usually with finned-tube condensers and necessarily with in-tube condensation. Although Liu and Cheng [109,110] and Kim et al. [232] studied the microchannel and in-tube dropwise condensation, the working fluid was water. Despite the fact that dropwise condensation of refrigerants on surfaces has also been studied [221], no experiments of refrigerants dropwise condensation in HVAC systems have been reported. The key issue is the difference in surface tension between the refrigerant and water by an order of magnitude, which is the critical factor in the formation of dropwise condensation. For example, air conditioning heat transfer is also impeded by condensing atmospheric water, which can accumulate on the coils causing degradation of heat transfer and corrosion of the coils. Therefore, it is necessary to develop durable surfaces with low surface energy and high mobility to realize refrigerant dropwise condensation.

6.4. Thermal management

With the rapid development of semiconductor technology, the integration and performance of electronic components continue to rise. The increasing power density has brought serious heat dissipation problems. If the electronic devices fail to dissipate heat timely, it will cause the local temperature of microelectronic devices to be too high, and the

operational performance and stability will be significantly reduced. Traditional cooling technology (such as air cooling, single-phase liquid cooling) can no longer meet the cooling requirements of the electronics industry. Microchannel heat dissipation, spray cooling, and heat pipe technologies have been increasingly used. Such phase change heat transfer technologies usually include an evaporation side and a condensation side as well as a return mechanism to bring the condensate back to the evaporator. However, this technique is similar to air cooling equipment where the thermal resistance on the air side is dominant. Consequently, it is not always advantageous to unilaterally promote the heat load in the condensate section. Nowadays, as the spontaneous jumping and directional migration behaviors of condensate droplets are discovered, a new mechanism for condensate return will be developed.

6.5. Petrochemical refining

According to the statistics, China's annual oil consumption in 2020 is over 700 million tons. Petroleum products are obtained by fractional distillation, which involves the evaporation and condensation of crude oil components. Usually, water is used as the cooling medium in shell and tube condensers. Although the applicability of dropwise condensation in distillation was mentioned in several published literatures, the enhanced effect was not quantitatively evaluated. Most importantly, it is unknown whether the distilled vapor can exist in the form of discrete droplets.

7. Conclusions and Outlook

This work reviews the recent process on droplet dynamics and condensation heat transfer on the advanced functional surfaces. The mechanism of solid-liquid interfacial interaction of droplet dynamics as well as enhancement strategies for condensation heat transfer has been well understood. Droplet dynamic characteristics and heat transfer performance in the process of condensation on advanced coatings as well as novel surfaces have been tested and evaluated. Droplet dynamics modulated by the variation of interfacial structure and operation conditions are closely related by droplet nucleation, growth, merging and detachment during dropwise condensation, and are also widely used in industrial applications, including energy utilization, desalination, pesticide spraying, power plants as well as HAVC. Recently, with the rapid development of nanotechnology and micro/nano machining, the precise construction of micro or nano structures has been implemented. The size range of droplet modulation is broadened and the condensation heat transfer performance is further improved.

Since the dynamic behaviors of droplets are accompanied by different scale spans, and the dynamic characteristics of droplets at different scales varies greatly. Therefore, the understanding of droplet wetting and dynamic behaviors has to take the characteristic scales where they are located into account. For example, it is impossible to achieve good and precise modulation of wetting and dynamic behaviors of droplets by nanostructure or micropillar arrays with single roughness, because the substrate structure is only capable of modulating droplets with similar size to its scale. In contrast, the hierarchical micro/nano structured surface allows for the simultaneous multiscale modulation of droplet growth, merging and departure. Besides, it not only maintains the condensate droplets in a stable Cassie state, but also can induce the droplet shedding rapidly at a smaller size. In addition, the effective combination of hydrophilic and hydrophobic surfaces has a synergistic effect on the modulation of droplets and liquid film, strengthening the nucleation of condensate droplets and simultaneously accelerating the droplets removal. The main research for the future is as follows: (1) droplet modulation at a specific scale is insufficient to meet the practical requirements. The combination of multiscale composite structures and hydrophobicity/hydrophilicity to investigate the synergistic modulation mechanism of droplets at different scales often achieve the unexpected results. Currently, the droplet modulation on the hierarchical micro/nano structures is limited to a small amount of experimental data, and it is necessary to develop a unified model to guide or optimize the design and fabrication of functional surfaces. (2) Different from macroscopic fluids, droplets show the significant difference scales. As the droplet size gradually decreases, the dominant role of bulk force such as inertial force is gradually replaced by viscous force and surface tension, so that the analysis of the droplet dynamics requires consideration of the balance of various forces. Moreover, coupled heat transfer is essential in condensation heat transfer, which has an extremely complexity and multiscale characteristics. Future investigations concentrate on developing a unified model to describe the solid-liquid interaction between droplets and micro/nano structured substrates during multiscale droplet modulation. (3) The modulation of droplet wetting states and dynamic behaviors in micro scale is still in its infancy. The wetting and dynamic theory for nanodroplets still requires further improvement to meet the current needs of the various applications.

Due to its multiscale characteristics, an in-depth understanding of dropwise condensation heat transfer under the influence of multiple factors is of great importance. Firstly, it is significant to gain insight into the mechanism of droplet nucleation in depth. The nucleation rate and spatial distribution play the significant role in the evolution of initial droplet formation and wetting behaviors. Although the restricted space caused by the hierarchical micro/nano structure is conducive to the nucleation process, it is difficult to provide a better insight limited by the current imaging technology. The second is the removal condensate droplets. With the continuous application of new removal methods such as external field strengthening or self-jumping of condensate droplets, it is one of the current difficulties to establish models for droplet departure under different conditions and the determination conditions for different droplet shedding modes. Although different numerical methods have been successful in their respective scales, the full-scale simulation of "nucleation-growth-coalescence-detachment" is also a challenge. As the functional hydrophobic coatings are applied in industry, the durability will be tested and the need for low preparation costs will be met. Future developments will focus on the following areas: (1) develop a new theory for dropwise condensation to achieve the prediction of heat transfer under the various operating conditions; (2) perform new numerical methods to implement full-scale simulations of the entire life cycle of dropwise condensation; and (3) combine the micro/nano structure with surface wettability to maintain the effective dropwise condensation or even droplet jumping condensation for a long operating time at a larger subcooling.

Credit author statement

Xin Wang: Conceptualization, Methodology, Investigation, Data curation, Writing original draft, Writing review & editing.

Bo Xu: Formal analysis, Funding acquisition, Investigation.

Zhenqian Chen: Writing original draft, Funding acquisition, Writing review & editing.

Dong Li: Conceptualization, Supervision, Writing review & editing.

Leigang Zhang: Conceptualization, Formal analysis, Investigation, Writing original draft.

Qiusheng Liu: Formal analysis, Funding acquisition, Investigation, Writing review & editing.

Yang Yang: Writing original draft, Formal analysis.

Qian Cao: Conceptualization, Supervision, Project administration.

Declaration of Competing Interest

I would like to declare on behalf of my co-authors that the work described was original research that has not been published previously, and not under consideration for publication elsewhere, in whole or in part. All the authors listed have approved the manuscript that is enclosed.

Acknowledgement

This work was supported by National Natural Science Foundation of China (Nos. 52006031, 52006107 and 52106116), ESA-CMSA International Cooperation of Space Experiment Project (Study on Condensation and Enhancement Methods under Microgravity) and Postgraduate Research & Practice Innovation Program of Jiangsu Province (KYCX21_0092).

References

[1] Young T. An essay on the cohesion of liquids. Phil. Trans. R. Soc. London 1805; 95:65–87.
[2] Rao DN. The concept, characterization, concerns and consequences of contact angles in solid-liquid-liquid systems. 3rd International Symposium on Contact Angle. Wettability and Adhesion 2003;3:191–210.
[3] Wenzel RN. Resistance of solid surfaces to wetting by water. Ind. Eng. Chem. 1936;28:988–94.
[4] Cassie ABD, Baxter S. Wettability of porous surfaces. Trans. Faraday Soc. 1944; 40:546–51.
[5] Cassie ABD. Contact angles. Discuss Faraday Soc 1948;3:11–6.
[6] Israelachvili JN, Gee ML. Contact angles on chemically heterogeneous surfaces. Langmuir 1989;5:288–9.
[7] Gao LC, McCarthy TJ. How Wenzel and Cassie were wrong? Langmuir 2007;23: 3762–5.
[8] Larsen ST, Taboryski RA. Cassie-like law using triple phase boundary line fractions for faceted droplets on chemically heterogeneous surfaces. Langmuir 2009;25:1282–4.
[9] Choi W, Tuteja A, Mabry JM, Cohen RE, McKinley GH. A modified Cassie-Baxter relationship to explain contact angle hysteresis and anisotropy on non-wetting textured surfaces. J. Colloid Interface Sci. 2009;339:208–16.
[10] Milne AJB, Amirfazli A. The Cassie equation: how it is meant to be used. Adv. Colloid Interf. Sci. 2012;170:48–55.
[11] Miwa M, Nakajima A, Fujishima A, Hashimoto K, Watanabe T. Effects of the surface roughness on sliding angles of water droplets on superhydrophobic surfaces. Langmuir 2000;16:5754–60.
[12] Marmur A. Wetting on hydrophobic rough surfaces: to be heterogeneous or not to be? Langmuir 2003;19:8343–8.
[13] Erbil HY, Cansoy CE. Range of applicability of the Wenzel and Cassie-Baxter equations for superhydrophobic surfaces. Langmuir 2009;25:14135–45.
[14] Wong TS, Ho CM. Dependence of macroscopic wetting on nanoscopic surface textures. Langmuir 2009;25:12851–4.
[15] Bormashenko E. General equation describing wetting of rough surfaces. J. Colloid Interface Sci. 2011;360:317–9.
[16] Bormashenko E. Wetting of real surfaces. Berlin: De Gruyter; 2013.
[17] Neumann AW, Good RJ. Thermodynamics of contact angles. I. Heterogeneous solid surfaces. J. Colloid Interface Sci. 1972;38:341–58.
[18] Marmur A. Soft contact: measurement and interpretation of contact angles. Soft Matter 2006;2:12–7.
[19] Bico J, Thiele U, Quéré D. Wetting of textured surfaces. Colloids Surf. A Physicochem. Eng. Asp. 2002;206:41–6.
[20] Ishino C, Okumura K, Quéré D. Wetting transitions on rough surfaces. Europhys. Lett. 2004;68:419–25.
[21] Boreyko JB, Chen CH. Self-propelled dropwise condensate on superhydrophobic surfaces. Phys. Rev. Lett. 2009;103:184501.
[22] Liu F, Ghigliotti G, Feng JJ, Chen CH. Numerical simulations of self-propelled jumping upon drop coalescence on non-wetting surfaces. J. Fluid Mech. 2014; 752:39–65.
[23] Wang X, Xu B, Chen Z, Yang Y, Cao Q. Effects of gravitational force and surface orientation on the jumping velocity and energy conversion efficiency of coalesced droplets. Microgravity Sci Tec 2020;32:1185–97.
[24] Wasserfall J, Figueiredo P, Kneer R, Rohlfs W, Pischke P. Coalescence-induced droplet jumping on superhydrophobic surfaces: Effects of droplet mismatch. Phys Rev Fluids 2017;2:123601.
[25] Eggers J, Lister JR, Stone HA. Coalescence of liquid drops. J. Fluid Mech. 1999; 401:293–310.
[26] Joseph DP, Justin CB, Sidney RN, Santosh A, Michael TH, Osman AB. The inexorable resistance of inertia determines the initial regime of drop coalescence. P Natl Acad Sci USA 2012;109:6857–61.
[27] Duchemin L, Eggers J, Josserand C. Inviscid coalescence of drops. J. Fluid Mech. 2003;487:167–78.
[28] Wu M. Scaling law in liquid drop coalescence driven by surface tension. Phys. Fluids 2004;16:51–4.
[29] Gao S, Liao Q, Liu W, Liu Z. Coalescence-induced jumping of nanodroplets on textured surfaces. J. Phys. Chem. Lett. 2018;9:13–8.
[30] Cha H, Xu C, Sotelo J, Chun JM, Yokoyama Y, Enright R, et al. Coalescence-induced nanodroplet jumping. Phys Rev Fluids 2016;1:064102.
[31] Wang X, Chen Z, Xu B. Coalescence-induced jumping of condensate droplets on microstructured surfaces with different gravitational fields by lattice Boltzmann method. Comput. Fluids 2019;188:60–9.
[32] Xie F, Wang D, Wang Y, Yang Y, Wang X. Coalescence-induced jumping of nanodroplets on mixed-wettability superhydrophobic surfaces. Can. J. Phys. 2021;99:297–301.
[33] Yin C, Wang T, Che Z, Jia M, Sun K. Critical and optimal wall conditions for coalescence-induced droplet jumping on textured superhydrophobic surfaces. Langmuir 2019;35:16201–9.
[34] Yuan Z, Wu X, Chu F, Wu R. Numerical simulations of guided self-propelled jumping of droplets on a wettability gradient surface. Appl. Therm. Eng. 2019; 156:524–30.
[35] Li H, Yang W, Aili A, Zhang T. Insights into the impact of surface hydrophobicity on droplet coalescence and jumping dynamics. Langmuir 2017;33:8574–81.
[36] Wang Y, Ming P. Dynamic and energy analysis of coalescence-induced self-propelled jumping of binary unequal-sized droplets. Phys. Fluids 2019;31: 122108.
[37] Liu C, Zhao M, Zheng Y, Lu D, Song L. Enhancement and guidance of coalescence-induced jumping of droplets on superhydrophobic surfaces with a U-groove. ACS Appl. Mater. Interfaces 2021;13:32542–54.
[38] Vahabi H, Wang W, Mabry JM, Kota AK. Coalescence-induced jumping of droplets on superomniphobic surfaces with macrotexture. Sci. Adv. 2018;4: eaau3488.
[39] Yan X, Zhang L, Sett S, Feng L, Zhao C, Huang Z, et al. Droplet jumping: effects of droplet size, surface structure, pinning, and liquid properties. ACS Nano 2019;13: 1309–23.
[40] Wang K, Ma X, Chen F, Lan Z. Effect of a superhydrophobic surface structure on droplet jumping velocity. Langmuir 2021;37:1779–87.
[41] Gao S, Hu Z, Yuan Z, et al. Flexible and efficient regulation of coalescence-induced droplet jumping on superhydrophobic surfaces with string. Appl. Phys. Lett. 2021;118:191602.
[42] Yuan Z, Gao S, Hu Z, Dai L, Hou H, Chu F, et al. Ultimate jumping of coalesced droplets on superhydrophobic surfaces. J. Colloid Interface Sci. 2021;587: 429–36.
[43] Wang X, Chen Z, Xu B. Coalescence-induced jumping of condensate droplets on microstructured surfaces with different gravitational fields by lattice Boltzmann method. Comput. Fluids 2019;188:60–9.
[44] Xie F, Wang D, Yang Y, Wang X, Lee DJ. Coalescence-induced jumping and condensation of argon nanodroplets in the Cassie or the Wenzel state on nanopillar-arrayed surfaces. Colloids Surf. A Physicochem. Eng. Asp. 2021;628: 127269.
[45] Xie F, Lu G, Wang X, Wang D. Enhancement of coalescence-induced nanodroplet jumping on superhydrophobic surfaces. Langmuir 2018;34:11195–203.
[46] Attarzadeh R, Dolatabadi A. Coalescence-induced jumping of micro-droplets on heterogeneous superhydrophobic surfaces. Phys. Fluids 2017;29:012104.
[47] Zhang L, Yuan W. A lattice Boltzmann simulation of coalescence-induced droplet jumping on superhydrophobic surfaces with randomly distributed structures. Appl. Surf. Sci. 2018;436:172–82.
[48] Lu D, Zhao M, Zhang H, Yang Y, Zheng Y. Self-enhancement of coalescence-induced droplet jumping on superhydrophobic surfaces with an asymmetric V-groove. Langmuir 2020;36:5444–53.
[49] Liu X, Cheng P. 3D multiphase lattice Boltzmann simulations for morphological effects on self-propelled jumping of droplets on textured superhydrophobic surfaces. Int Commun Heat Mass 2015;64:7–13.
[50] Vahabi H, Wang W, Davies S, Mabry JM, Kota AK. Coalescence-induced self-propulsion of droplets on superomniphobic surfaces. ACS Appl. Mater. Interfaces 2017;9:29328–36.
[51] Farokhirad S, Morris JF, Lee T. Coalescence-induced jumping of droplet: Inertia and viscosity effects. Phys. Fluids 2015;27:102102.
[52] Farokhirad S, Mohammadi SM, Lee T. Coalescence-induced jumping of immersed and suspended droplets on microstructured substrates. Eur J Comput Mech 2017; 26:205–23.
[53] Chen Y, Lian Y. Numerical investigation of coalescence-induced self-propelled behavior of droplets on non-wetting surfaces. Phys. Fluids 2018;30:112102.
[54] Chen X, Weibel JA, Garimella SV. Characterization of coalescence-induced droplet jumping height on hierarchical superhydrophobic surfaces. ACS Omega 2017;2:2883–90.
[55] Enright R, Miljkovic N, Sprittles J, Nolan K, Mitchell R, Wang EN. How coalescing droplets jump. ACS Nano 2014;8:10352–62.
[56] Zhu Y, Tso CY, Ho TC, Leung MK, Yao S. Coalescence-induced jumping droplets on nanostructured biphilic surfaces with contact electrification effects. ACS Appl. Mater. Interfaces 2021;13:11470–9.
[57] Chen X, Patel RS, Weibel JA, Garimella SV. Coalescence-induced jumping of multiple condensate droplets on hierarchical superhydrophobic surfaces. Sci. Rep. 2016;6:1–11.
[58] Shi Y, Tang G, Xia H. Investigation of coalescence-induced droplet jumping on superhydrophobic surfaces and liquid condensate adhesion on slit and plain fins. Int. J. Heat Mass Transf. 2015;88:445–55.
[59] Chu F, Yuan Z, Zhang X, Wu X. Energy analysis of droplet jumping induced by multi-droplet coalescence: The influences of droplet number and droplet location. Int. J. Heat Mass Transf. 2018;121:315–20.
[60] Xing D, Wang R, Wu F, Gao X. Confined growth and controlled coalescence/self-removal of condensate microdrops on a spatially heterogeneously patterned superhydrophilic- superhydrophobic Surface. ACS Appl. Mater. Interfaces 2020; 12:29946–52.
[61] Gao S, Liao Q, Liu W, Liu Z. Self-removal of multiple and multisize coalescing nanodroplets on nanostructured surfaces. J. Phys. Chem. C 2018;122:20521–6.
[62] Wang K, Liang Q, Jiang R, Zheng Y, Lan Z, Ma X. Numerical simulation of coalescence-induced jumping of multidroplets on superhydrophobic surfaces: initial droplet arrangement effect. Langmuir 2017;33:6258–68.

[63] Wang Y, Ming P. Coalescence-induced self-propelled jumping of three droplets on non-wetting surfaces: Droplet arrangement effects. J. Appl. Phys. 2021;129:014702.
[64] Yuan Z, Hu Z, Gao S, Wu X. The effect of the initial state of the droplet group on the energy conversion efficiency of self-propelled jumping. Langmuir 2019;35:16037–42.
[65] Peng Q, Yan X, Li J, Li L, Cha H, Ding Y, et al. Breaking droplet jumping energy conversion limits with superhydrophobic microgrooves. Langmuir 2020;36:9510–22.
[66] Wang K, Li R, Liang Q, Jiang R, Zheng Y, Lan Z, et al. Critical size ratio for coalescence-induced droplet jumping on superhydrophobic surfaces. Appl. Phys. Lett. 2017;111:061603.
[67] Xie F, Lu G, Wang X, Wang B. Coalescence-induced jumping of two unequal-sized nanodroplets. Langmuir 2018;34:2734–40.
[68] Wang Y, Ming P. Effect of radius ratios of two droplets on coalescence-induced self-propelled jumping. AIP Adv. 2018;8:065320.
[69] Chaudhury MK, Whitesides GM. Correlation between Surface Free Energy and Surface Constitution. Science 1992;255:1230–2.
[70] Whitesides GM, Chaudhury MK. How to make water run uphill. Science 1992;256:1539–41.
[71] Daniel S, Chaudhury MK, Chen JC. Fast drop movements resulting from the phase change on a gradient surface. Science 2001;291:633–6.
[72] Daniel S, Chaudhury MK, De Gennes PG. Vibration-actuated drop motion on surfaces for batch microfluidic processes. Langmuir 2005;21:4240–8.
[73] Daniel S, Chaudhury MK. Rectified motion of liquid drops on gradient surfaces induced by vibration. Langmuir 2002;18:3404–7.
[74] Wang H. Motion of droplets and dropwise condensation on the gradient surface. Chongqing University Press; 2008.
[75] Yamada R, Tada H. Manipulation of droplets by dynamically controlled wetting gradients. Langmuir 2005;21:4254–6.
[76] Lai Y, Yang J, Shieh D. A microchip fabricated with a vapor-diffusion self-assembled-monolayer method to transport droplets across superhydrophobic to hydrophilic surfaces. Lab Chip 2010;10:499–504.
[77] Paradisanos I, Fotakis C, Anastasiadis SH, Stratakis E. Gradient induced liquid motion on laser structured black Si surfaces. Appl. Phys. Lett. 2015;107:111603.
[78] Ghosh A, Ganguly R, Schutzius TM, Megaridis CM. Wettability patterning for high-rate, pumpless fluid transport on open, non-planar microfluidic platforms. Lab Chip 2014;14:1538–50.
[79] Deng S, Shang W, Feng S, Zhu S, Xing Y, Hou Y, et al. Controlled droplet transport to target on a high adhesion surface with multi-gradients. Sci. Rep. 2017;7:45687.
[80] Chowdhury IU, Sinha Mahapatra P, Sen AK. Self-driven droplet transport: Effect of wettability gradient and confinement. Phys. Fluids 2019;31:042111.
[81] Li Z, Hu G, Wang Z, Ma YB, Zhou ZW. Three dimensional flow structures in a moving droplet on substrate: A dissipative particle dynamics study. Phys. Fluids 2013;25:072103.
[82] Chakraborty M, Chowdhury A, Bhusan R, DasGupta S. Molecular Dynamics Study of Thermally Augmented Nanodroplet Motion on Chemical Energy Induced Wettability Gradient Surfaces. Langmuir 2015;31:11260–8.
[83] Pravinraj T, Patrikar R. Modelling and investigation of partial wetting surfaces for drop dynamics using lattice Boltzmann method. Appl. Surf. Sci. 2017;409:214–22.
[84] Lee JS, Moon JY, Lee JS. Study of transporting of droplets on heterogeneous surface structure using the lattice Boltzmann approach. Appl. Therm. Eng. 2014;72:104–13.
[85] Deng Z, Zhang C, Shen C, Cao J, Chen Y. Self-propelled dropwise condensation on a gradient surface. Int. J. Heat Mass Transf. 2017;114:419–29.
[86] Zheng Y, Cheng J, Zhou C, Xing H, Wen X, Pi P, et al. Droplet motion on a shape gradient surface. Langmuir 2017;33:4172–7.
[87] Hiltl S, Böker A. Wetting phenomena on (gradient) wrinkle substrates. Langmuir 2016;32:8882–8.
[88] Wu J, Ma R, Wang Z, Yao S. Do droplets always move following the wettability gradient? Appl. Phys. Lett. 2011;98:204104.
[89] Liu C, Sun J, Li J, Xiang C, Che L, Wang Z, et al. Long-range spontaneous droplet self-propulsion on wettability gradient surfaces. Sci. Rep. 2017;7:1–8.
[90] Xu C, Jia Z, Lian X. Wetting and adhesion energy of droplets on wettability gradient surfaces. J. Mater. Sci. 2020;55:8185–98.
[91] Yin X, Wang D, Liu Y, Yu B, Zhou F. Controlling liquid movement on a surface with a macro-gradient structure and wetting behavior. J. Mater. Chem. A 2014;2:5620–4.
[92] Khoo HS, Tseng FG. Spontaneous high-speed transport of subnanoliter water droplet on gradient nanotextured surfaces. Appl. Phys. Lett. 2009;95:063108.
[93] Mertaniemi H, Jokinen V, Sainiemi L, Franssila S, Marmur A, Ikkala O, et al. Superhydrophobic tracks for low-friction, guided transport of water droplets. Adv. Mater. 2011;23:2911–4.
[94] Yang X, Song J, Zheng H, Deng X, Liu X, Lu X, et al. Anisotropic sliding on dual-rail hydrophilic tracks. Lab Chip 2017;17:1041–50.
[95] Alwazzan M, Egab K, Peng B, Khan J, Li C. Condensation on hybrid-patterned copper tubes (I): Characterization of condensation heat transfer. Int. J. Heat Mass Transf. 2017;112:991–1004.
[96] Yang KS, Lin KH, Tu CW, He YZ, Wang CC. Experimental investigation of moist air condensation on hydrophilic, hydrophobic, superhydrophilic, and hybrid hydrophobic-hydrophilic surfaces. Int. J. Heat Mass Transf. 2017;115:1032–41.
[97] Ghosh A, Beaini S, Zhang BJ, Ganguly R, Megaridis CM. Enhancing dropwise condensation through bioinspired wettability patterning. Langmuir 2014;30:13103–15.
[98] Chatterjee A, Derby MM, Peles Y, Jensen MK. Enhancement of condensation heat transfer with patterned surfaces. Int. J. Heat Mass Transf. 2014;71:675–81.
[99] Rose JW. Dropwise condensation theory and experiment: a review. Proc Inst Mech Eng A J Power Energy 2002;216:115–28.
[100] El Fil B, Kini G, Garimella S. A review of dropwise condensation: Theory, modeling, experiments, and applications. Int. J. Heat Mass Transf. 2020;160:120172.
[101] Ma J, Sett S, Cha H, Yan X, Miljkovic N. Recent developments, challenges, and pathways to stable dropwise condensation: A perspective. Appl. Phys. Lett. 2020;116:260501.
[102] Zheng S, Gross U, Wang X. Dropwise condensation: From fundamentals of wetting, nucleation, and droplet mobility to performance improvement by advanced functional surfaces. Adv. Colloid Interf. Sci. 2021;295:102503.
[103] Kim S, Kim KJ. Dropwise condensation modeling suitable for superhydrophobic surfaces. J. Heat Transf. 2011;133:081502.
[104] Miljkovic N, Enright R, Wang EN. Modeling and optimization of superhydrophobic condensation. J. Heat Transf. 2013;135:111004.
[105] Maeda Y, Lv F, Zhang P, Takata Y, Orejon D. Condensate droplet size distribution and heat transfer on hierarchical slippery lubricant infused porous surfaces. Appl. Therm. Eng. 2020;176:115386.
[106] Wu WH, Maa JR. A mechanism for dropwise condensation and nucleation. Chem. Eng. J. 1976;11:143–6.
[107] Le Fevre J, Rose JW. A theory of heat transfer by dropwise condensation. In: Proceedings of the 3rd International Heat Transfer Conference. 2; 1966. p. 362–75.
[108] Abu-Orabi M. Modeling of heat transfer in dropwise condensation. Int. J. Heat Mass Transf. 1998;41:81–7.
[109] Liu X, Cheng P. Dropwise condensation theory revisited: part I. droplet nucleation radius. Int. J. Heat Mass Transf. 2015;83:833–41.
[110] Liu X, Cheng P. Dropwise condensation theory revisited Part II. Droplet nucleation density and condensation heat flux. Int. J. Heat Mass Transf. 2015;83:842–9.
[111] Xie J, Xu J, Shang W, Zhang K. Dropwise condensation on superhydrophobic nanostructure surface, part II: Mathematical model. Int. J. Heat Mass Transf. 2018;127:1170–87.
[112] Xie J, She Q, Xu J, Liang C, Li W. Mixed dropwise-filmwise condensation heat transfer on biphilic surface. Int. J. Heat Mass Transf. 2020;150:119273.
[113] Xu Z, Zhang L, Wilke KL, Wang EN. Modeling of jumping-droplet condensation with dynamic droplet growth. In: Proceedings of the 16th International Heat Transfer Conference; 2018. p. 5073–80.
[114] Zheng S, Eimann F, Philipp C, Fieback T, Gross U. Modeling of heat and mass transfer for dropwise condensation of moist air and the experimental validation. Int. J. Heat Mass Transf. 2018;120:879–94.
[115] Singh M, Kondaraju S, Bahga SS. Mathematical model for dropwise condensation on a surface with wettability gradient. J. Heat Transf. 2018;140:071502.
[116] Shang Y, Hou Y, Yu M, Yao S. Modeling and optimization of condensation heat transfer at biphilic interface. Int. J. Heat Mass Transf. 2018;122:117–27.
[117] Kimura T, Maruyama S. Molecular dynamics simulation of heterogeneous nucleation of a liquid droplet on a solid surface. Microscale Thermophys Eng 2002;6:3–13.
[118] Sheng Q, Sun J, Wang Q, Wang W, Wang H. On the onset of surface condensation: formation and transition mechanisms of condensation mode. Sci. Rep. 2016;6:1–9.
[119] Niu D, Tang G. The effect of surface wettability on water vapor condensation in nanoscale. Sci. Rep. 2016;6:1–6.
[120] Niu D, Gao H, Tang G, Yan Y. Droplet nucleation and growth in the presence of noncondensable gas: A molecular dynamics study. Langmuir 2021;37:9009–16.
[121] Niu D, Gao H, Yan Y. A discussion for the formation of cassie droplet on nanostructured surface using molecular dynamics simulation. Case Stud Therm Eng 2021;25:100976.
[122] Huang D, Quan X, Cheng P. An investigation on vapor condensation on nanopillar array surfaces by molecular dynamics simulation. Int Commun Heat Mass 2018;98:232–8.
[123] Tang G, Niu D, Guo L, Xu J. Failure and Recovery of Droplet Nucleation and Growth on Damaged Nanostructures: A Molecular Dynamics Study. Langmuir 2020;36:13716–24.
[124] Gao S, Liao Q, Liu W, Liu W. Effects of solid fraction on droplet wetting and vapor condensation: a molecular dynamic simulation study. Langmuir 2017;33:12379–88.
[125] Ranathunga DTS, Shamir A, Dai X, Nielsen SO. Molecular Dynamics Simulations of Water Condensation on Surfaces with Tunable Wettability. Langmuir 2020;36:7383–91.
[126] Xu B, Chen Z. Molecular dynamics study of water vapor condensation on a composite wedge-shaped surface with multi wettability gradients. Int Commun Heat Mass 2019;105:65–72.
[127] Liu X, Cheng P. Lattice Boltzmann simulation of steady laminar film condensation on a vertical hydrophilic subcooled flat plate. Int. J. Heat Mass Transf. 2013;62:507–14.
[128] Liu X, Cheng P. Lattice Boltzmann simulation for dropwise condensation of vapor along vertical hydrophobic flat plates. Int. J. Heat Mass Transf. 2013;64:1041–52.
[129] Li X, Cheng P. Lattice Boltzmann simulations for transition from dropwise to filmwise condensation on hydrophobic surfaces with hydrophilic spots. Int. J. Heat Mass Transf. 2017;110:710–22.
[130] Zhang C, Cheng P, Minkowycz WJ. Lattice Boltzmann simulation of forced condensation flow on a horizontal cold surface in the presence of a non-condensable gas. Int. J. Heat Mass Transf. 2017;115:500–12.

[131] Guo Q, Cheng P. 3D lattice Boltzmann investigation of nucleation sites and dropwise-to-filmwise transition in the presence of a non-condensable gas on a biomimetic surface. Int. J. Heat Mass Transf. 2019;128:185–98.
[132] Li Q, Luo K, Li X. Forcing scheme in pseudopotential lattice Boltzmann model for multiphase flows. Phys. Rev. E 2012;86:016709.
[133] Li Q, Kang Q, Francois MM, He Y, Luo K. Lattice Boltzmann modeling of boiling heat transfer: The boiling curve and the effects of wettability. Int. J. Heat Mass Transf. 2015;85:787–96.
[134] Li M, Huber C, Mu Y, Tao W. Lattice Boltzmann simulation of condensation in the presence of noncondensable gas. Int. J. Heat Mass Transf. 2017;109:1004–13.
[135] Shen L, Tang G, Li Q, Shi Y. Hybrid wettability-induced heat transfer enhancement for condensation with noncondensable gas. Langmuir 2019;35:9430–40.
[136] Wang X, Xu B, Chen Z, Yang Y, Cao Q. Lattice Boltzmann modeling of condensation heat transfer on downward-facing surfaces with different wettabilities. Langmuir 2020;36:9204–14.
[137] Wang X, Xu B, Chen Z, Yang Y, Cao Q. Lattice Boltzmann simulation of dropwise condensation on the microstructured surfaces with different wettability and morphologies. Int. J. Therm. Sci. 2021;160:106643.
[138] Wang X, Chang J, Chen Z, Xu B. Mesoscopic lattice Boltzmann simulation of droplet jumping condensation heat transfer on the microstructured surface. Int Commun Heat Mass 2021;127:105567.
[139] Wang X, Xu B, Liu Q, Yang Y, Chen Z. Enhancement of vapor condensation heat transfer on the micro-and nano-structured superhydrophobic surfaces. Int. J. Heat Mass Transf. 2021;177:121526.
[140] Shi Y, Tang G, Shen L. Study of coalescence-induced droplet jumping during phase-change process in the presence of noncondensable gas. Int. J. Heat Mass Transf. 2020;152:119506.
[141] Bortolin S, Da Riva E, Del Col D. Condensation in a square minichannel: application of the VOF method. Heat Transfer Eng 2014;35:193–203.
[142] Yin Z, Guo Y, Sunden B, Wang Q, Zeng M. Numerical simulation of laminar film condensation in a horizontal minitube with and without non-condensable gas by the VOF method. Numer Heat Tr A-Appl 2015;68:958–77.
[143] Da Riva E, Del Col D. Numerical simulation of laminar liquid film condensation in a horizontal circular minichannel. J. Heat Transf. 2012;134:051019.
[144] Lei Y, Chen Z. Numerical study of condensation flow regimes in presence of non-condensable gas in minichannels. Int Commun Heat Mass 2019;106:1–8.
[145] Lee H, Son G. Level-set based numerical simulation of film condensation in a vertical downward channel flow. Int Commun Heat Mass 2018;95:171–81.
[146] Lee H, Son G. Numerical and analytical study of laminar film condensation in upward and downward vapor flows. Numer Heat Tr A-Appl 2018;74:1139–53.
[147] Lee WH. A pressure iteration scheme for two-phase flow modeling. In: Veziroglu TN, editor. Multiphase Transport Fundamentals, Reactor Safety, Applications. DC: Hemisphere Publishing Washington; 1980.
[148] Ke Z, Shi J, Zhang B, Chen CL. Numerical investigation of condensation on microstructured surface with wettability patterns. Int. J. Heat Mass Transf. 2017;115:1161–72.
[149] Jiang J, Liu F, Zhang X, Wei H. Model development and simulation on dropwise condensation by coupling absorption theory in the presence of non-condensable gas (NCG). Int Commun Heat Mass 2020;119:104936.
[150] Hu Z, Yuan Z, Hou H, Chu F, Wu X. Event-driven simulation of multi-scale dropwise condensation. Int. J. Heat Mass Transf. 2021;167:120819.
[151] Macner AM, Daniel S, Steen PH. Simulating heat transfer during transient dropwise condensation on a low-thermal-conductivity substrate. Langmuir 2019;35:11566–78.
[152] Rose JW, Glicksman LR. Dropwise condensation-the distribution of drop sizes. Int. J. Heat Mass Transf. 1973;16:411–25.
[153] Edwards JA, Doolittle JS. Tetrafluoroethylene promoted dropwise condensation. Int. J. Heat Mass Transf. 1965;8:663–6.
[154] Marto PJ, Looney DJ, Rose JW, Wanniarachchi AS. Evaluation of organic coatings for the promotion of dropwise condensation of steam. Int. J. Heat Mass Transf. 1986;29:1109–17.
[155] Tsuchiya H, Manabe K, Gaudelet T, Moriya T, Suwabe K, Tenjimbayashi M, et al. Improvement of heat transfer by promoting dropwise condensation using electrospun polytetrafluoroethylene thin films. New J. Chem. 2017;41:982–91.
[156] Budakli M, Salem TK, Arik M, Donmez B, Menceloglu Y. Effect of polymer coating on vapor condensation heat transfer. J. Heat Transf. 2020;142:041602.
[157] Ma X, Wang B, Xu D, Lin J. Lifetime test of dropwise condensation on polymer-coated surfaces. Heat Transf Asian Res 1999;28:551–8.
[158] Ma X, Chen J, Xu D, Lin J, Ren C, Long Z. Influence of Surface Properties of Polymer Film on Dropwise Condensation Heat Transfer. J Chem Ind Eng China 2002;53:1221–6.
[159] Paxson AT, Yagüe JL, Gleason KK, Varanasi KK. Stable dropwise condensation for enhancing heat transfer via the initiated chemical vapor deposition (iCVD) of grafted polymer films. Adv. Mater. 2014;26:418–23.
[160] Khalil K, Soto D, Farnham T, Paxson A, Katmis AU, Gleason K, et al. Grafted nanofilms promote dropwise condensation of low-surface-tension fluids for high-performance heat exchangers. Joule 2019;3:1377–88.
[161] Damle VG, Sun X, Rykaczewski K. Can Metal Matrix-Hydrophobic Nanoparticle Composites Enhance Water Condensation by Promoting the Dropwise Mode. Adv. Mater. Interfaces 2015;2:1500202.
[162] Chang HC, Rajagopal MC, Hoque MJ, Oh J, Li L, Li J, et al. Composite structured surfaces for durable dropwise condensation. Int. J. Heat Mass Transf. 2020;156:119890.
[163] Yang Q, Gu A. Dropwise condensation on SAM and electroless composite coating surfaces. J Chem Eng Japan 2006;39:826–30.
[164] Ma J, Cha H, Kim MK, Cahill DG, Miljkovic N. Condensation induced delamination of nanoscale hydrophobic films. Adv. Funct. Mater. 2019;29:1905222.
[165] Woodruff DW, Westwater JW. Steam condensation on various gold surfaces. J. Heat Transf. 1981;103:685–92.
[166] Smith T. The hydrophilic nature of a clean gold surface. J. Colloid Interface Sci. 1980;75:51–5.
[167] Ge M, Wang S, Zhao J, Zhao Y, Liu L. Effects of extended surface and surface gold plating on condensation characteristics of steam with large amount of CO_2. Exp. Thermal Fluid Sci. 2018;92:13–9.
[168] O'Neill GA, Westwater JW. Dropwise condensation of steam on electroplated silver surfaces. Int. J. Heat Mass Transf. 1984;27:1539–49.
[169] Gore GB, Sali NV, Ghodake AB. Of dropwise condensation heat transfer enhancement on silver coated copper surface using n-Heptane as surfactant additive. Int Adv Res J Sci Eng Technol 2016;3:291–4.
[170] Azimi G, Dhiman R, Kwon HM, Paxson AT, Varanasi KK. Hydrophobicity of rare-earth oxide ceramics. Nat. Mater. 2013;12:315–20.
[171] Khan S, Azimi G, Yildiz B, Varanasi KK. Role of surface oxygen-to-metal ratio on the wettability of rare-earth oxides. Appl. Phys. Lett. 2015;106:061601.
[172] Shim J, Seo D, Oh S, Lee J, Nam Y. Condensation heat-transfer performance of thermally stable superhydrophobic cerium-oxide surfaces. ACS Appl. Mater. Interfaces 2018;10:31765–76.
[173] Das A, Kilty HP, Marto PJ, Kumar A, Andeen GB. Dropwise condensation of steam on horizontal corrugated tubes using an organic self-assembled monolayer coating. J Enhanc Heat Transf 2000;7:109–23.
[174] Yang Q, Gu A. Dropwise condensation on SAM and electroless composite coating surfaces. J Chemical Eng Japan 2006;39:826–30.
[175] Chandekar A, Sengupta SK, Whitten JE. Thermal stability of thiol and silane monolayers: A comparative study. Appl. Surf. Sci. 2010;256:2742–9.
[176] Das AK, Kilty HP, Marto PJ, Andeen GB, Kumar A. The use of an organic self-assembled monolayer coating to promote dropwise condensation of steam on horizontal tubes. J. Heat Transf. 2000;122:278–86.
[177] Wen R, Lan Z, Peng B, Xu W, Ma X, Cheng Y. Droplet departure characteristics and dropwise condensation heat transfer at low steam pressure. J. Heat Transf. 2016;138:071501.
[178] Vemuri S, Kim KJ, Wood BD, Govindaraju S, Bell TW. Long term testing for dropwise condensation using self-assembled monolayer coatings of n-octadecyl mercaptan. Appl. Therm. Eng. 2006;26:421–9.
[179] Bonner RW. Dropwise condensation life testing of self assembled monolayers. 14th Int Heat Transf Conf 2010:221–6.
[180] Xue C, Ma J. Long-lived superhydrophobic surfaces. J. Mater. Chem. A 2013;1:4146–61.
[181] Li Y, Li L, Sun J. Bioinspired self-healing superhydrophobic coatings. Angew. Chem. Int. Ed. 2010;122:6265–9.
[182] Preston DJ, Mafra DL, Miljkovic N, Kong J, Wang EN. Scalable graphene coatings for enhanced condensation heat transfer. Nano Lett. 2015;15:2902–9.
[183] Han JT, Kim SY, Woo JS, Lee GW. Transparent, conductive, and superhydrophobic films from stabilized carbon nanotube/silane sol mixture solution. Adv. Mater. 2008;20:3724–7.
[184] Bayer IS, Steele A, Loth E. Superhydrophobic and electroconductive carbon nanotube- fluorinated acrylic copolymer nanocomposites from emulsions. Chem. Eng. J. 2013;221:522–30.
[185] Zhu L, Xiu Y, Xu J, Tamirisa PA, Hess DW, Wong CP. Superhydrophobicity on two-tier rough surfaces fabricated by controlled growth of aligned carbon nanotube arrays coated with fluorocarbon. Langmuir 2005;21:11208–12.
[186] Kumar GU, Krishnan DV, Suresh S, Thansekhar MR, Prasanna RV, Jubal M. Investigating the combined effect of square microgrooves and CNT coating on condensation heat transfer. Appl. Surf. Sci. 2019;469:50–60.
[187] Chen CH, Cai Q, Tsai C, Chen CL, Xiong G, Yu Y, et al. Dropwise condensation on superhydrophobic surfaces with two-tier roughness. Appl. Phys. Lett. 2007;90:173108.
[188] Kim MS, Ada KAL, Kwon OK, Park CW. A comparison of condensation heat transfer performance of MWCNT/Fe composite coatings on steel substrate. J. Mech. Sci. Technol. 2014;28:1589–96.
[189] Starostin A, Valtsifer V, Barkay Z, Legchenkova I, Danchuk V, Bormashenko E. Drop-wise and film-wise water condensation processes occurring on metallic micro-scaled surfaces. Appl. Surf. Sci. 2018;444:604–9.
[190] Sharma CS, Stamatopoulos C, Suter R, von Rohr PR, Poulikakos D. Rationally 3D-textured copper surfaces for Laplace pressure imbalance-induced enhancement in dropwise condensation. ACS Appl. Mater. Interfaces 2018;10:29127–35.
[191] Zhu J, Luo Y, Tian J, Li J, Gao X. Clustered ribbed-nanoneedle structured copper surfaces with high-efficiency dropwise condensation heat transfer performance. ACS Appl. Mater. Interfaces 2015;7:10660–5.
[192] Feng S, Delannoy J, Malod A, Zheng H, Quéré D, Wang Z. Tip-induced flipping of droplets on Janus pillars: From local reconfiguration to global transport. Sci. Adv. 2020;6:eabb4540.
[193] Miljkovic N, Enright R, Nam Y, Lopez K, Dou N, Sack J, et al. Jumping-droplet-enhanced condensation on scalable superhydrophobic nanostructured surfaces. Nano Lett. 2013;13:179–87.
[194] Miljkovic N, Wang EN. Condensation heat transfer on superhydrophobic surfaces. MRS Bull. 2013;38:397–406.
[195] Wen R, Lan Z, Peng B, Xu W, Yang R, Ma X. Wetting transition of condensed droplets on nanostructured superhydrophobic surfaces: coordination of surface properties and condensing conditions. ACS Appl. Mater. Interfaces 2017;9:13770–7.

[196] Mulroe MD, Srijanto BR, Ahmadi SF, Collier CP, Boreyko JB. Tuning superhydrophobic nanostructures to enhance jumping-droplet condensation. ACS Nano 2017;11:8499–510.
[197] Xie J, Xu J, Li X, Liu H. Dropwise condensation on superhydrophobic nanostructure surface, Part I: Long-term operation and nanostructure failure. Int. J. Heat Mass Transf. 2019;129:86–95.
[198] Wen R, Li Q, Wu J, Wu G, Wang W, Chen Y, et al. Hydrophobic copper nanowires for enhancing condensation heat transfer. Nano Energy 2017;33:177–83.
[199] Wen R, Xu S, Ma X, Lee YC, Yang R. Three-dimensional superhydrophobic nanowire networks for enhancing condensation heat transfer. Joule 2018;2:269–79.
[200] Lu MC, Lin CC, Lo CW, Huang CW, Wang CC. Superhydrophobic Si nanowires for enhanced condensation heat transfer. Int. J. Heat Mass Transf. 2017;111:614–23.
[201] Wang R, Wu F, Xing D, Yu F, Gao X. Density maximization of one-step electrodeposited copper nanocones and dropwise condensation heat-transfer performance evaluation. ACS Appl. Mater. Interfaces 2020;12:24512–20.
[202] Wang R, Wu F, Yu F, Zhu J, Gao X, Jiang L. Anti-vapor-penetration and condensate microdrop self-transport of superhydrophobic oblique nanowire surface under high subcooling. Nano Res. 2021;14:1429–34.
[203] Jin Y, Qamar A, Shi Y, Wang P. Preferential water condensation on superhydrophobic nano-cones array. Appl. Phys. Lett. 2018;113:211601.
[204] Chen X, Wu J, Ma R, Hua M, Koratkar N, Yao S, et al. Nanograssed micropyramidal architectures for continuous dropwise condensation. Adv. Funct. Mater. 2011;21:4617–23.
[205] Chen X, Weibel JA, Garimella SV. Exploiting microscale roughness on hierarchical superhydrophobic copper surfaces for enhanced dropwise condensation. Adv. Mater. Interfaces 2015;2:1400480.
[206] Chen X, Li Q, Hou K, Li X, Wang Z. Microflower-decorated superhydrophobic copper surface for dry condensation. Langmuir 2019;35:16275–80.
[207] Aili A, Li H, Alhosani MH, Zhang T. Unidirectional fast growth and forced jumping of stretched droplets on nanostructured microporous surfaces. ACS Appl. Mater. Interfaces 2016;8:21776–86.
[208] Xie J, Xu J, He X, Liu Q. Large scale generation of micro-droplet array by vapor condensation on mesh screen piece. Sci. Rep. 2017;7:1–13.
[209] Yan X, Chen F, Sett S, Chavan S, Li H, Feng L, et al. Hierarchical condensation. ACS Nano 2019;13:8169–84.
[210] Lo CW, Chu YC, Yen MH, Lu MC. Enhancing condensation heat transfer on three-dimensional hybrid surfaces. Joule 2019;3:2806–23.
[211] Chen S, Wang R, Wu F, Zhang H, Gao X, Jiang L. Copper-based high-efficiency condensation heat transfer interface consisting of superhydrophobic hierarchical microgroove and nanocone structure. Mater Today Phys 2021;19:100407.
[212] Peng Q, Jia L, Guo J, Dang C, Ding Y, Yin L, et al. Forced jumping and coalescence-induced sweeping enhanced the dropwise condensation on hierarchically microgrooved superhydrophobic surface. Appl. Phys. Lett. 2019;114:133106.
[213] Lv C, Hao P, Yao Z, Song Y, Zhang X, He F. Condensation and jumping relay of droplets on lotus leaf. Appl. Phys. Lett. 2013;103:021601.
[214] Feng S, Delannoy J, Malod A, Zheng H, Quéré D, Wang Z. Tip-induced flipping of droplets on Janus pillars: From local reconfiguration to global transport. Sci. Adv. 2020;6:eabb4540.
[215] Parker AR, Lawrence CR. Water capture by a desert beetle. Nature 2001;414:33–4.
[216] Hou Y, Yu M, Chen X, Wang Z, Yao S. Recurrent filmwise and dropwise condensation on a beetle mimetic surface. ACS Nano 2015;9:71–81.
[217] Ju J, Bai H, Zheng Y, Zhao T, Fang R, Jiang L. A multi-structural and multi-functional integrated fog collection system in cactus. Nat. Commun. 2012;3:1–6.
[218] Wong TS, Kang SH, Tang SKY, Smythe EJ, Hatton BD, Grinthal A, et al. Bioinspired self-repairing slippery surfaces with pressure-stable omniphobicity. Nature 2011;477:443–7.
[219] Anand S, Paxson AT, Dhiman R, Smith JD, Varanasi KK. Enhanced condensation on lubricant-impregnated nanotextured surfaces. ACS Nano 2012;6:10122–9.
[220] Xiao R, Miljkovic N, Enright R, Wang EN. Immersion condensation on oil-infused heterogeneous surfaces for enhanced heat transfer. Sci. Rep. 2013;3:1–6.
[221] Sett S, Sokalski P, Boyina K, Li L, Rabbi KF, Auby H, et al. Stable dropwise condensation of ethanol and hexane on rationally designed ultrascalable nanostructured lubricant-infused surfaces. Nano Lett. 2019;19:5287–96.
[222] Guo L, Tang G. Dropwise condensation on bioinspired hydrophilic-slippery surface. RSC Adv. 2018;8:39341–51.
[223] Dai X, Sun N, Nielsen SO, Stogin BB, Wang J, Yang S, et al. Hydrophilic directional slippery rough surfaces for water harvesting. Sci. Adv. 2018;4:eaaq0919.
[224] Miljkovic N, Preston DJ, Enright R, Wang EN. Electrostatic charging of jumping droplets. Nat. Commun. 2013;4:1–9.
[225] Miljkovic N, Preston DJ, Enright R, Wang EN. Electric-field-enhanced condensation on superhydrophobic nanostructured surfaces. ACS Nano 2013;7:11043–54.
[226] Traipattanakul B, Tso CY, Chao CYH. Electrostatic-induced coalescing-jumping droplets on nanostructured superhydrophobic surfaces. Int. J. Heat Mass Transf. 2019;128:550–61.
[227] Wikramanayake ED, Bahadur V. Electrowetting-based enhancement of droplet growth dynamics and heat transfer during humid air condensation. Int. J. Heat Mass Transf. 2019;140:260–8.
[228] Migliaccio CP. Resonance-induced condensate shedding for high-efficiency heat transfer. Int. J. Heat Mass Transf. 2014;79:720–6.
[229] Oh I, Cha H, Chen J, Chavan S, Kong H, Miljkovic N, et al. Enhanced condensation on liquid-infused nanoporous surfaces by vibration-assisted droplet sweeping. ACS Nano 2020;14:13367–79.
[230] Zhao Q, Burnside BM. Dropwise condensation of steam on ion implanted condenser surfaces. Heat Recovery Syst CHP 1994;14:525–34.
[231] Kananeh AB, Rausch MH, Fröba AP, Leipertz A. Experimental study of dropwise condensation on plasma-ion implanted stainless steel tubes. Int. J. Heat Mass Transf. 2006;49:5018–26.
[232] Kim DE, Ahn HS, Kwon TS. Experimental investigation of filmwise and dropwise condensation inside transparent circular tubes. Appl. Therm. Eng. 2017;110:412–23.